The Role of Surfactants in Gas Hydrate Management

Jyoti Shanker Pandey, Adam Paul Karcz, and Nicolas von Solms

Abstract This chapter provides an introductory understanding of the role of surfactants in the formation of gas hydrates. The main theories that have been developed over the past decades are discussed with support from computational aspects that have become increasingly useful in this regard. Particularly for surfactants, the structure-property relations are key in the full understanding of their behavior in the context of hydrate formation kinetics and equilibria, which are presented with evidence from various studies. Furthermore, surfactants can benefit from co-promoters that may be utilized in hydrate formation, so we present some details to highlight the importance of their interactions. More recently, bio-based surfactants have gained interest out of environmental concerns, and we showcase some of the most interesting cases of their implementation. Although there have been many examples of how gas hydrates can be used for cold storage, hydrogen storage, and other industrial applications, the usage of surfactants or other additives has not been well supported with clear fundamental understandings. Thus, there have been endeavors to gain these insights via computational tools that span different scales, like quantum mechanics and molecular dynamic simulations. The use of these tools is explained with examples. Combining all these different aspects, we hope to provide some understanding of the role of surfactants in current and emerging hydrate management technologies.

J. S. Pandey · N. von Solms (✉)
Center for Energy Resource Engineering (CERE), Department of Chemical Engineering, Technical University of Denmark, 2800 Kgs. Lyngby, Denmark
e-mail: nvs@kt.dtu.dk

A. P. Karcz
Department of Energy Conversion and Storage, Solid State Chemistry, Technical University of Denmark, 2800 Kgs. Lyngby, Denmark

T. Solling et al. (eds.), *Surfactants in Upstream E&P*, Petroleum Engineering,
https://doi.org/10.1007/978-3-030-70026-3_15

1 Introduction

Gas hydrates are ice-like crystalline compounds having different guest molecules surrounded by water cages formed at high pressure but low temperature conditions. These hydrates look like ice; however, they have different physical and chemical properties [1]. The guest molecules could be gases, such as small molecules (e.g., CH_4 or CO_2) or large molecules like propane. Guest molecules are entrapped and stabilized within cages due to intermolecular forces, and cages are formed by water molecules connected to each other via hydrogen bonding. Based on three-dimensional orientation, the hydrate structure can be divided into three types: s-I, s-II, and s-H. Gas hydrate formation is a crystallization process which occurs in different stages, mainly nucleation, growth and agglomeration [2]. Gas hydrates can store a large volume of gas such that 1 m^3 of hydrate volume can store up to 163 m^3 of gas. Gas hydrates also offer additional advantages over conventional gas storage technologies, such as being environmentally friendly, non-explosive, and low mantainence. Gas hydrates applications can be divided into four categories with respect to their origin and application, represented in Fig. 1.

Gas hydrates are found in nature within sediments and are considered a source of gas supply for future generation. These untouched gas hydrate reservoirs are in the continental shelf in the marine environment as well as cold regions on land, such as permafrost regions in Alaska, Canada, China, and Russia. It is estimated that these reservoirs contain 1.5×10^{16} m^3 of gas [3, 4]. Hydrates are also believed to present on other planets, including Mars and Saturn [5]. Gas hydrates formation in oil and gas pipeline is considered an engineering challenge in the petroleum industry as hydrate formation could block and damage the pipelines [6, 7]. Studies in this context are focused on preventing hydrate formation by injecting chemicals known has hydrate inhibitors. Based on the mechanism, these inhibitors are categorized as high dosage thermodynamic hydrate inhibitors (THI, 20–40 wt%) and low dosage hydrate inhibitors (LDHI, 0.1–5 wt%). Due to environmental impact consideration,

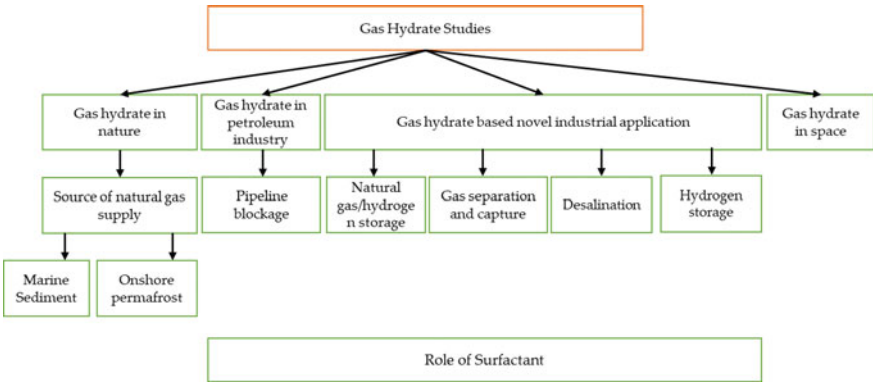

Fig. 1 Role of surfactant in different gas hydrate based applications

LDHI is used more frequently than THI [8]. The most common surfactants used under LDHI type are quaternary ammonium surfactants characterized having n-butyl or n-pentyl functional groups and long alkyl chains [9].

Opposite to hydrate inhibitors, a different class of chemicals, known as promoters, improve formation kinetics needed in different industrial applications [10], such as natural gas storage [11], hydrogen storage [12], hydrate-based pre- and post-combustion CO_2 separation, capture, storage, transport [13–15], and hydrate-based desalination [16].

During laboratory-based hydrate studies, gas hydrate is formed at gas-water interface as gas solubility in water is slow and gas saturated water is crystallization process is very slow to happen. A thin hydrate layer forms first at gas-liquid interface which later grows towards the gas phase; however, growth is limited by mass transfer of gas molecule through the thin hydrate layer [17]. To move toward commercialization, the kinetics of gas hydrate formation require drastic improvement. This could be achieved through mechanical techniques as well as adding surface-active chemicals that could reduce the mass transfer barrier and enhance the gas-liquid contact area without changing the hydrate phase equilibrium [18]. These surface-active agents are used in small concentrations and known as hydrate promoters. Surfactants [19] and hydrophobic amino acids [20] are known to be hydrate promoters. Recently low dosage methanol is also considered as hydrate promoter due to its near similar behaviour as a surfactant at low concentration [21].

This chapter is focused on discussing the role of surfactants as surface-active agents during gas hydrate formation and dissociation. Formation kinetics depends on guest molecule, pressure, temperature, and reactor design. Surfactant performance is also system-dependent, including the difference in reactor design, pressure, and temperature conditions, the difference in hydrate forming gas mixture as well as the role of supporting material due to difference in thermal conductivity and surface-to-volume ratio [22–24]. In this chapter, we discuss the available mechanisms and current status of surfactant application in gas hydrate management briefly.

2 Role of Surfactant Molecular Structure on Hydrate Promotion

Surfactants are known to affect the kinetics of the hydrate formation. Kinetics of hydrate formation can be divided into different stages, starting from dissolution, nucleation, growth, and agglomeration [1]. Surfactants facilitate faster nucleation by reducing the surface free energy by absorbing into the aqueous-hydrocarbon (gas/liquid) interface [25]. Surfactants also enhance the mass transfer by improving the hydrocarbon solubility into the water. Surfactants play an essential role at the gas-liquid and liquid-hydrate interface. A surfactant could occupy the area at the interface and could also hinder hydrate formation. In this context, sodium dodecyl sulfate is considered to be the most effective surface-active agent to enhance nucleation

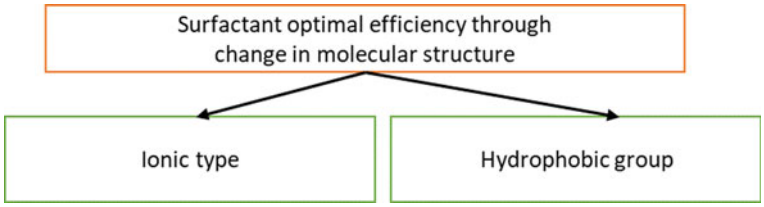

Fig. 2 Role of molecular structure of surfactant optimal efficiency during gas hydrate formation

and growth phases [26–28]. Surfactants are composed of hydrophobic "tails" and hydrophilic headgroups within a single molecule, which determine the surfactant properties. Surfactant molecules could diffuse from the bulk phase to the liquid-gas interface, such that the hydrophilic end stays in the liquid phase while the hydrophobic end stays in the gas phase. This would lead to a change in surface tension, modification in contact angle, and change in surface charge and surface viscosity [29]. At a given concentration, surfactant molecules bind together in different shapes and orientations, called micelles [30]. Above the critical micelle concentration (CMC), the hydrophilic part covers the hydrophobic group and supports the organic compound (methane or CO_2) solubility [31]. Surfactants are well used chemical substances to enhance surface activity that control spreadability, wetting, foaming, etc. [19]; however, it is still unclear about the key mechanism responsible and the role of concentration during formation mechanism. Insights into the molecular structure of surfactant can enhance our understanding of its role in hydrate formation kinetics. The key component of the surfactant structure is given in Fig. 2.

2.1 Ionic Type

Surfactants tested for hydrate formation are from anionic, cationic, and nonionic natures. Studies confirmed that anionic surfactants produced better promotion compared to cationic and nonionic ones at lower concentration (100–500 ppm). At higher concentration (>800 ppm), the difference in promotion ability decreased [32, 33]. Among three homologuous anionic surfactants, Sodium dodecyl sulfate (SDS), Sodium tetradecyl sulfate (STS) and Sodium hexadecyl sulfate (SHS), it was found that SDS is most effective above 1000 ppm concentration for methane hydrate formation while STS has shown same promotion behaviour at 100 ppm [34]. SHS was not effective compared to SDS and SHS. In another study on the comparative performance of different surfactants (anionic/cationic/nonionic) during CO_2 hydrate formation, anionic surfactant SDS was the most effective among all three. Nonionic surfactants are more effective compared to cationic surfactant [35]. In another study, when *n*-dodecyltrimethylammonium chloride (DTAC) and Tween 20 were used for the Tetrahydrofuran (THF/H_2) system and THF/Methane system, both surfactants showed different behavior. This led to the conclusion that the role of surfactant during

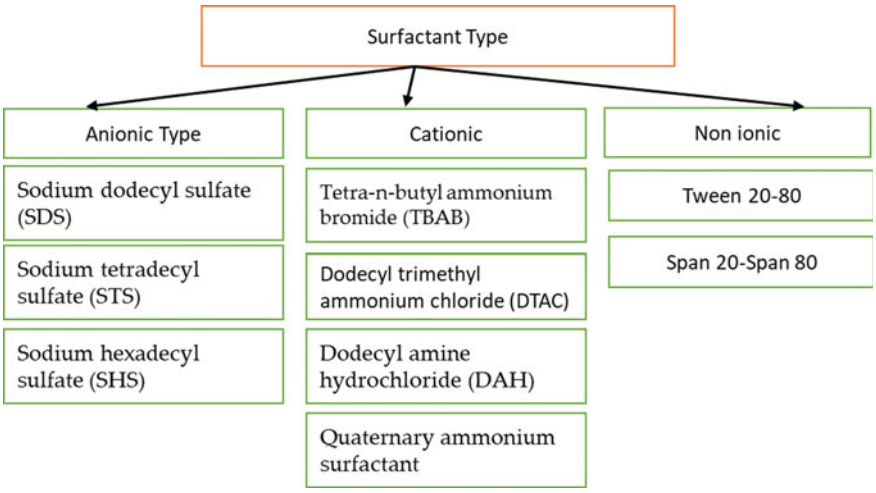

Fig. 3 Popular surfactans used in gas hydrate studies

hydrate formation is dependent on guest molecules as well as the system (single guest molecule vs. mixed hydrate) [36]. Figure 3 provides the details of the key surfactant in each category. Apart from traditional classification, novel surfactants, including biosurfactants and Gemini surfactant, have also been used in hydrate-based studies [37–39]. Figure below describe some popular surfactants used frequently in gas hydrate studies.

2.2 Properties of Hydrophobic Group

Size of the hydrophobic and hydrophilic groups controls the surfactant properties, such as interfacial tension. Large groups have lower interfacial tension than smaller groups [40, 41] Properties of the hydrophobic group affect the surfactant properties and are of greater research interest [42]. Kumar et al. [19] have provided a summary of the properties of the hydrophobic group and their effect on the surfactant properties. Three key elements include the change in the length of the hydrophobic group, branching, and unsaturation in the hydrophobic group and the presence of an aromatic nucleus in the hydrophobic group. The hydrophobic group-controlled solubility of surfactant in water and organic solvent, biodegradability and packing of surfactant at the interface. With an increase in the length of the hydrophobic group, the solubility of surfactant in water decreases, but in organic solvent it increases. Apart from that, biodegradability and surfactant absorption at the interface also increases as the length of the hydrophobic part increases [19]. Okutani et al. [34] studied the effect of alkyl chain length, using three surfactants (SDS, STS, and SHS) having the same headgroup ($-OSO_3-Na^+$) but different carbon chains (12, 14, or 16, respectively).

They concluded that surfactant with larger carbon number could be useful even at lower concentrations. On the other hand, Dicharry et al. [43] have tested the effect of carbon chain for sulphate-based surfactants and found out that higher carbon chain-based surfactants could readily absorb on hydrate surfaces by forming hemimicelles, hence promoting hydrate formation. The difference in carbon chain length creates different solubility and packing area. By looking at the available research, it can be concluded that sulphate-/sulfonate-based surfactants have shown the best promotion capabilities with 12–14 carbon chain as an optimal solution. As per adsorption and mass transfer theory, an increase in chain length could decrease the surfactant hydrate promotion efficiencies.

3 General Theories Behind the Surfactant-Based Promotion

Kalogerakis et al. [18] were one of the first to study the role of surfactants during hydrate formation. During nucleation, hydrate film formed at the gas-liquid interface, which further isolates gas phase from the liquid phase and allows only gas molecule reaching to liquid phase through diffusion. The exact mechanism behind the role of surfactant during hydrate formation is not yet agreed upon. Many theories have been proposed. In the following section, we have discussed some well-known theories available in the literature and describe in the Fig. 4 [31].

3.1 Micelles Formation Theory

In one notable research proposing micelles theory, critical micelle concentration (CMC) was reported as 242 ppm using SDS during natural gas hydrate formation

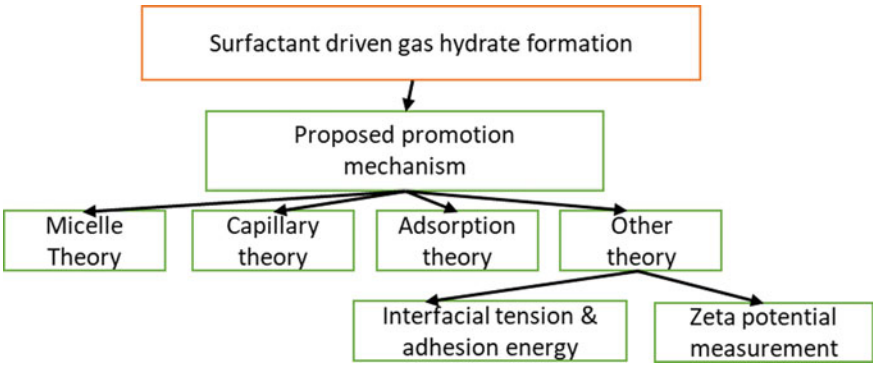

Fig. 4 Surfactant based key hydrate formation theories

[28]. Experiments also suggest that the CMC value of natural gas-water solution decreases as the pressure decreases [28]. Other studies suggested that when surfactant SDS concentration was above the CMC, a 700-fold increase in the rate of hydrate formation was observed due to enhanced guest molecule solubilities [44]. Change in gas solubility due to change in surfactant concentration was also measured for the ethylene and SDS system, both at ambient pressure and under hydrate formation conditions [45]. Solubility behavior for ethylene and methane was similar under hydrate formation conditions in the presence of SDS [46]. Presence of CMC for SDS during methane hydrate formation was also confirmed [47]. The CMC-based hydrate formation mechanism is explained in the figure below. However, some researchers have disputed this theory, and citing that a decrease in the rate of methane hydrate formation above CMC was also observed for cationic and anionic surfactants [48, 49]. Few studies also suggested that SDS at even very low concentration (10 ppm) could promote methane hydrate formation [17] or a single molecule itself can assist in hydrate formation [50]. In another study, it was observed that the CMC value of surfactant does not depend on the hydrate formation conditions and remains unchanged [51].

3.2 Capillary Driven Growth

Presence of capillary action during hydrate formation was demonstrated by Watanabe et al. using SDS and Difluoromethane (HFC-32) gas [52]. Visual observation suggested that crystals were initially formed both at the liquid-gas interface as well as reactor sidewall at different spots. Thereafter, when crystals grew in size, coalesence took place with each other, and crystals started to grow at the reactor sidewall. After that, hydrate grew in a downward direction in the solution phase to maintain contact and cause a decrease in the solution surface. Additionally, rippling motion of liquid at the reactor wall also confirmed the presence of capillary action during the formation. Other studies also confirmed moving of gas-liquid interface in upward direction along the reactor wall in the presence of SDS and did not change the hydrate thermodynamics [17, 53]. This behaviour was not observed in the absence of surfactant for the pure water-gas system.

The capillary mechanism is said to be caused by either change in hydrate morphology [54–56] or due to change in the wettability [57–60]. Wang et al. have used anionic surfactants SDS, Sodium dodecyl benzene sulfonate (SDBS) and Sodium dodecyl sulfonate (SDSN) having different wettability on the reactor side and found that SDBS performed poorly compared to other surfactants due to weaker wettability on the reactor wall [60]. Wang et al. [59] have also achieved directional hydrate growth by controlling and varying the wettability of the solid surface inside the glass tube. Wettability of surfactant solution is also controlled by surfactant concentration. SDS wettability also changed due to the difference in its concentration [57]. NMR and Raman studies also confirmed that SDS has two different growth mechanisms at 25 ppm and 500 ppm. At higher concentration, water converted into an intermediate

solid-state and then combined with methane gas. This was not observed at the lower concentration [61].

The key limitation of this theory is that most of the observations regarding the capillary mechanism are for anionic surfactants, including SDS, STS, and SHS [34, 53] and for specific guest molecules, methane and ethane. In the presence of the CO_2 molecule and an anionic surfactant such as SDS, no capillary mechanism was observed at high driving force [62]. Other studies involving various surfactants, such as lithium dodecyl sulfate (LDS), dodecyl benzene sulfonic acid (DBSA), sodim oleate (SO), dodecyl alcohol ethoxylates (AEO), cetyltrimethylammonium bromide (CTAB) from cationic and non-ionic categories, did not confirm the capillary mechanism responsible for hydrate growth [63–65]. Therefore, it can be concluded that capillary-based hydrate growth is dependent on surfactant type, surfactant concentration, and guest molecules. For example, Molokitina et al [62] performed microscopic investigation of the CO_2 hydrate formation mechanism in bulk water phase in the presence of SDS under different mass transfer barrier and visualized the hydrate growth pattern as shown in Fig. 5. It can be seen that driving force changes the mechanism of gas hydrate formation at the gas/liquid interface, such that capillary-driven movement is observed at low driving force. Further research is required to understand the factors influencing the capillary mechanism and how this mechanism could be improved to achieve enhanced growth.

3.3 Adsorption Theory

Theory of surfactant adsorption on the hydrate surface was first proposed based on zeta potential measurements [66, 67] and is proposed as a cause behind improved hydrate formation kinetics [26, 66, 68]. Different types of surfactants were absorbed through a different mechanism and due to difference in surfactant concentration. For example, an ionic surfactant is considered to absorb on the hydrate surface under the influence of electrostatic forces while a non-ionic surfactant adsorbs through hydrogen bonding [69]. At concentrations below the CMC, adsorption behavior follows Henry's law, confirmed by Scamerhorn et al. [70]. Above the CMC, surfactants form hemimicelles which are an aggregate form of surfactant due to tail-tail interactions between surfactant molecules. Also above the CMC, adsorption is independent of the concentration [71].

3.4 Interfacial Tension and Adhesion Energy

This theory is based on the few studies that suggest that during the gas hydrate formation, the contact angle between the liquid-gas interface and solid-state change in the presence of the surfactant [53, 72]. Addition of surfactant decreases the surface tension of the aqueous phase, thus decreasing the contact angle. This causes creation

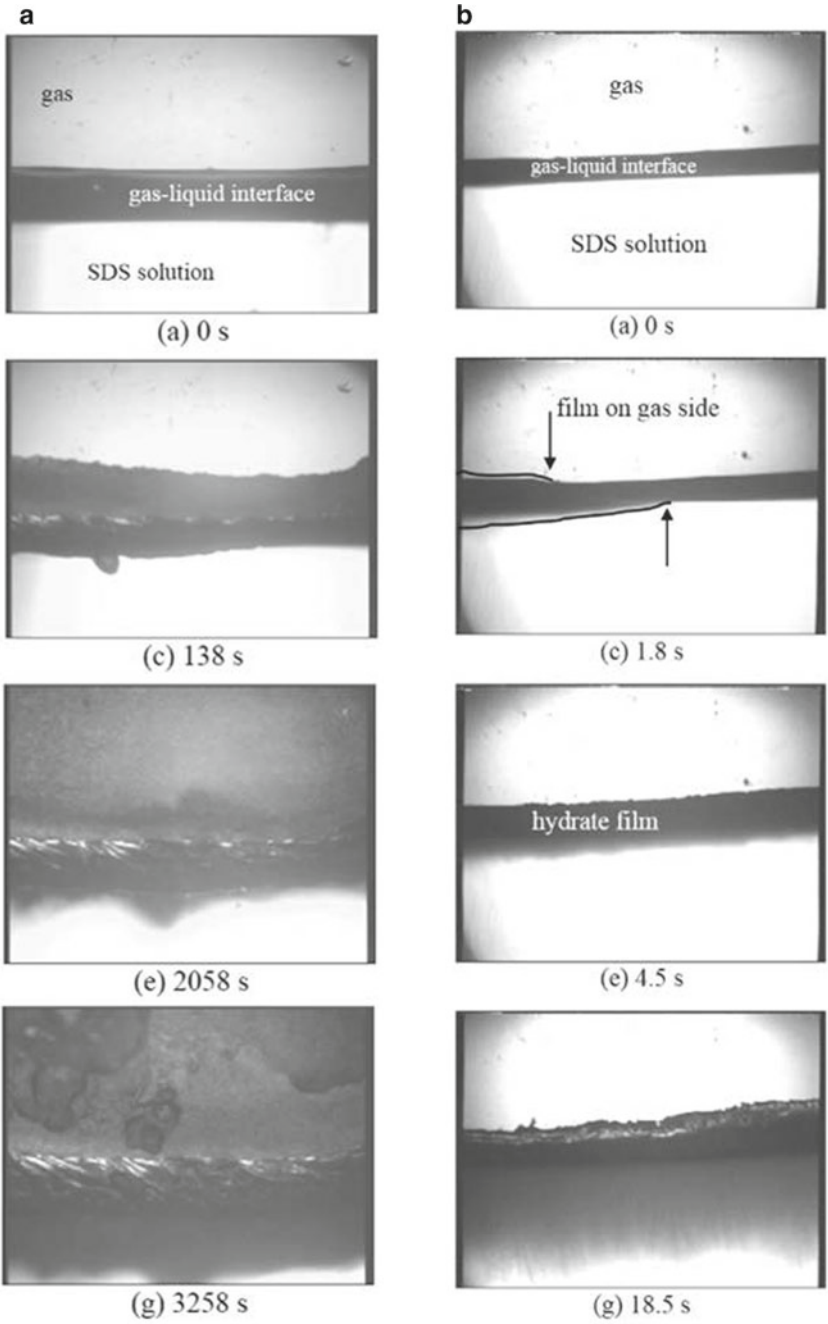

Fig. 5 **a** CO_2 hydrate film propagation along the gas-liquid interface (capillary-driven) in the presence of SDS (1000 ppm) and low mass transfer driving force. **b** CO_2 hydrate film propagation along the gas-liquid interface on both gas and liquid sides under high mass transfer driving force (not capillary-driven) in the presence of SDS (1000 ppm) [62]

of a film-like interface along the reactor wall and becomes a preferred location for hydrate nucleation and growth [53]. In the presence of surfactant, the solid surface becomes more water-wet due to the decrease in surface tension [72]. Song et al. suggested that the reduction in contact force and interfacial tension due to the presence of surfactant caused enhance hydrate growth [73].

3.5 Zeta Potential Measurement

Zeta potential measurement was used to explain the synergy between THF and SDS as reported by Torre et al. [74] for gas hydrate based CO_2 capture studies. In another study, Torre er al. [75] has suggested no mass transfer barrier was observed during the gas to liquid mass transfer in the presence of both SDS and SDS+THF. Zeta potential measurement has suggested that in the mixture of SDS and THF, THF hydrate stays dispersed due to electrostatic repulsion caused by adsorption of DS- anions on the hydrate surface hence porous texture allow CO_2 diffusion into the liquid phase [67].

During our recent study focused on kinetics of methane hydrate formation in the presence of SDS and effect of SDS concentration on the formation kinetics. We observed change in formation kinetic behavior around 2000–3000 ppm concentration. To suggested that behavior can be explained in terms of dual effect of absorption and surface tension. Trend in key kinetic properties as a function of SDS concentration is illustrated in Figs. 6 and 7 [47].

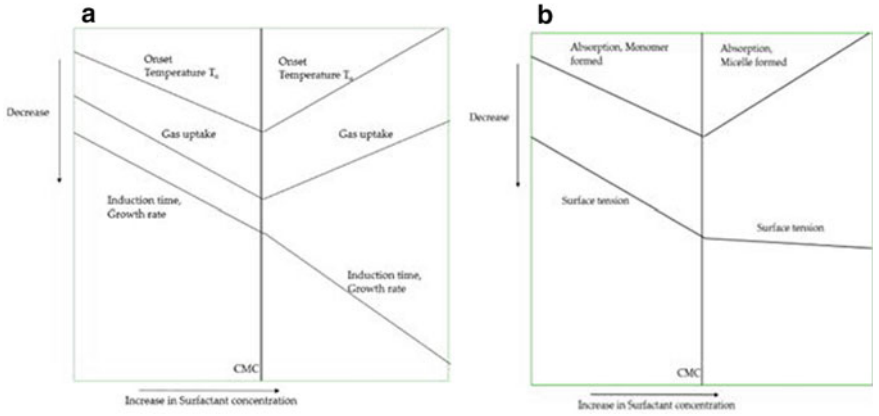

Fig. 6 **a** Key kinetic properties trend during methane hydrate formation as a function of SDS concentration (500-3000 ppm). Experimental observation confirm the presence of CMC between 2000–3000 ppm [47]. **b** Effect of change in SDS concentration on the absorption and surface tension (500–3000 ppm) [47]

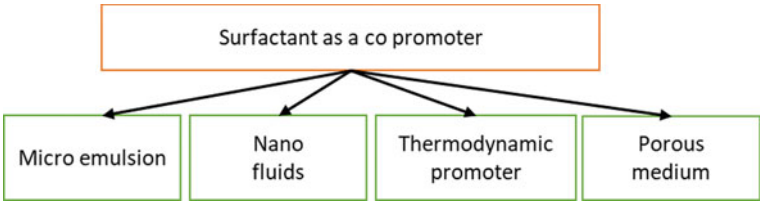

Fig. 7 Different association of surfactants as copromoter

4 Role of Surfactant with Co-promoting Gas Hydrate Formation

Surfactants have also played a key role as co promoter along with different agents and medium to enhance and stablise hydrate formation. Figure below describe their key associations.

4.1 Microemulsions

Surfactants also serve as supports for other systems that could achieve rapid hydrate formation, including microemulsions [76, 77], dry water, and nanofluids. In water-in-oil emulsions, methane molecules disperse into the oil phase and later diffuse and reach the water droplet surface to react. Each water droplet serves as an isolated nucleation front, thus able to create highly efficient water-to-hydrate conversion. Many factors, such as pressure, temperature, stirring, and initial water volume, control the stability and droplet size of the emulsion. Water cut controls not only the gas-liquid contact interface but also controls the water droplet size [78–81]. There are some challenges, such as hydrate film formation at the water droplet surface could retard gas transfer into water droplet, as well as formation and dissociation cycles could potentially destabilize the hydrate [82, 83].

4.2 Nano-Fluids

Nano-fluids are seen as the potential alternative to accelerate gas hydrate formation due to their superior thermal conductivity that addresses the exothermic and thermal inhibition during formation [84, 85]. Among different nanofluids, metal nanofluids such as silver nanoparticles have been tested repeatedly. Silver nanoparticles have been used to study methane and ethane hydrate nucleation and improvement in gas uptake, and the induction time was recorded. It is suggested that nanoparticles help during formation by providing nucleation sites, reducing effective interfacial tension and wetting angle between hydrate and particle [86–88]. A key challenge

during the application of nanoparticles for gas hydrate formation and dissociation is their stability during cycling. This could destroy nanoparticle stability and, thus, reusability. To stabilized nanoparticles, surfactants such as SDS are also used. SDS in low concentration has been used along with Al_2O_3-, ZnO-, CuO-based nanoparticles [89–91].

4.3 Thermodynamic Promoters

During the last decade, much attention has been placed on non-mechanical techniques to improve gas uptake and reduce nucleation time and the stochastic nature of hydrate nucleation and formation. These non-mechanical techniques consist of using chemicals categorized into kinetic and thermodynamic promoters. Thermodynamic promoters allow hydrate formation at moderate pressure and temperature condition by reducing the required formation pressure and increasing the temperature, making them sought for novel hydrate-based industrial applications. Frequently used thermodynamic promoters include tetrahydrofuran (THF), Tetra n-butyl ammonium bromide (TBAB), and cyclopentane (CP). The key disadvantage of using thermodynamic promoters includes loss of gas uptake due to the occupancy of the cages by the promoter molecule and slower formation kinetics. To overcome these challenges, surfactants such as SDS have been used along with thermodynamic promoters, including THF and CP, and have received greater attention due to more efficient performance compared to thermodynamic promoters.

Kumar et al. [92] have studied the role of SDS and THF on formation and dissociation kinetics of the methane hydrate in an unstirred reactor configuration. Their results concluded that SDS and THF could provide optimal configuration for methane hydrate storage and transportation at atmospheric pressure. Veluswamy et al. [93] used SDS (100 ppm) with THF (5.6 mol%) to achieve methane hydrate formation within 1 h at ambient temperature 293.2 K and 7.2 MPa. They also highlighted the synergetic effect between SDS and THF was visible only at ambient temperature. When the temperature was reduced to 283.2 K, the addition of SDS decreased the gas uptake by 20% and 60% at 72 bar and 30 bar, respectively. Mech et al. [94] also studied SDS along with THF and TBAB at 276.15 K and different pressures from 30 bar to 75 bar in a stirred tank reactor. They concluded that SDS at 600 ppm concentration, THF plus SDS had higher uptake at 75 bar while TBAB plus SDS had higher gas uptake at 30 bar. Kakati et al. [95] had tested the mixture of SDS and THF on the mixture of methane, ethane and propane and found that a THF and SDS combined system can be used to improve formation and thermodynamics of the natural gas storage in the form of the hydrates.

Additionally, SDS is used with another thermodynamic promoter in applications such as gas separation, CO_2 capture, desalination, and hydrogen energy storage, and it is further discussed in §5.

4.4 Porous Medium

Pan et al. [96] have discussed the presence of a porous medium and SDS on formation kinetics. Presence of porous medium improve the heat transfer as well as greater higher surface area leads to quicker 2D nucleation. It is usually challenging to form methane hydrate in the porous medium as a porous medium act as a thermodynamic inhibitor and controlled by the pore size and salinity [97]. It is general practice to add surfactant to enhance the kinetics of hydrate formation [17] however, the surfactant may influence wettability as well as can create an air bubble during gas injection; therefore, the surfactants have been ignored traditionally during the modelling of the hydrate formation process. Presence of surfactant leads to enhanced formation rate and much higher gas uptake. Results suggest that both particle size and water saturation play an important role in the hydrate formation kinetics. Particle size control interface-specific area, pore volume and pore size distribution whereas water saturation control water migration as well as hydrate distribution which intern controls formation and dissociation kinetics [96]. Addition of the surfactant in the liquid phase lowers the mass transfer resistance at the gas-liquid interface and reduce the surface tension. SDS, in particular, found effective because of hydrophobic active groups in the ionized SDS which would accumulate around the surface of the silica sand to avoid any contact with water in the solution. Many surfactant micelles are formed that further help methane dissolves more due to micelle solubilization [98]. In another study for SDS and water system, the presence of SDS increase the ethane hydrate dissociation rate and weaken the self-preservation tendency of the gas hydrate [99]. Some of the key research results are summarized in Table 1.

Amino acids are seen as eco friendly replacement of surfactant for gas hydrate based research and hydrophobic amino acids are seen as good alternative of SDS. Figures 8 and 9 compare the kinetics of methane hydrate formation between SDS and Amino acids at same concentration (3000 ppm) in different sands with four different sand particle sizes.

5 Application of Surfactant

Surfactants have been used as both as inhibitors as well as promoter in different industries and application and their usage is summarize in Fig. 10.

5.1 Surfactant-Based Hydrate Inhibition

Quaternary ammonium surfactants in low dosage amount are used as anti-agglomeration (AA) compounds for hydrate inhibition [9] to avoid hydrate plug formation in oil and gas pipelines. AA compounds form a well-structured thin layer

Table 1 Key experimental work focused on the kinetics of hydrate formation in the presence of porous media and surfactant

Gases	Porous medium	Promoter	Key observation	Ref.
CO_2	Silica gels (mesh size: 60–120, 100–200 and 230–400)	Tween-80, SDS (50, 2000 and 4000 ppm), DTAC	Dispersed liquid phase in pore space. Enhanced mass transfer	[35]
	Multi-walled carbon nanotubes (MWCNT), hydroxylated MWCNT, carboxylated MWCNT (COOH-MWCNT) (0.005–0.1 wt%)	SDS (0.03 wt%)	No effect on CO_2 hydrate phase equillbrium in the presence of nano fluids. 0.01 and 0.05 wt% COOH-MWCNT in the presence of 0.03 wt% SDS achieved maximum hydrate formation rate	[100]
	Nanoparticles of Al_2O_3 (0.1–0.6 wt%), cerium oxide (CeO_2), silicon dioxide (SiO_2) (0.1 wt%)	THF (7.8, 10 and 20 wt%), SDS (0.05–0.8 wt%)	CO_2 hydrate formation rate increased by 3.74 times in the presence of 0.6 wt% and 0.2 wt% Al_2O_3 Presence of 10 wt% THF into 0.6 wt% and 0.2 wt% Al_2O_3 results into optimum performance	[101]
CO_2 (80.6%) + N_2 (19.4%)	Soda glass BZ-01 (0.105–0.125 mm), BZ-02 (0.177–0.250 mm), BZ-04 (0.350–0.500 mm)	THF (3 mol%), SDS (1000 mg L^{-1})	Induction time τind and equllibirum (Peq) and were reduced by 3-mol% THF and 1000-mg L–1 SDS	[102]
CH_4	Fixed bed Alumina & Silica particles (2 mm–6 mm)	SDS (300 ppm)	Smaller particle size lead to larger gas uptake and lower induction time. Gas uptake is larger when alumnia particles are present. Presence of SDS increased the storage capacity in porous media 2-4 times compare to pure water case	[103]

(continued)

Table 1 (continued)

Gases	Porous medium	Promoter	Key observation	Ref.
CH_4	Four type silica sand Sand 1(46.4–245 μm) Sand 2 (160–630 μm) Sand 3 (480–1800 μm) Sand 4 (1400–5000 μm)	SDS (500-3000 ppm) Amino acids (3000 ppm)	Increase in particle size lead to lower induction time and lower gas uptake when the initial water saturation is 35% or above due to pore filling hydrate morphology	[104]

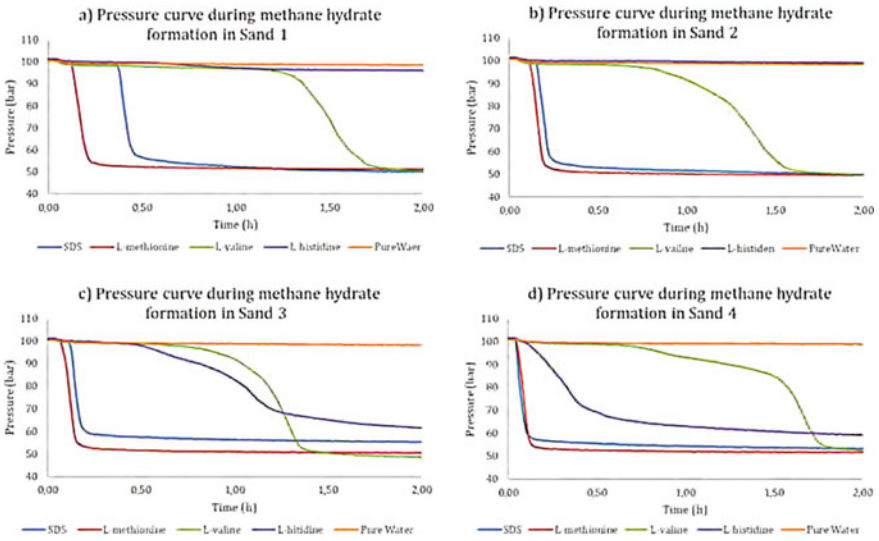

Fig. 8 Pressure variation during isothermal experiments at 100 bar and 1°C starting condition comparing the methane hydrate formation kinetics for SDS and four selected amino acids (L-valine, L-methinonine, L- histidine, L-arginine). Results suggest that SDS and L-methionine hydrate promotion capabilities are near similar in porous medium with different physical properties [104]

that further slows down hydrate aggregation and stops the crystal growth process due to mass transfer barrier [105, 106]. The thin layer could be formed either between water and oil or oil and hydrates and containssurfactants and alkanes from the oil phase [107–110]. Apart from ionic surfactants, Sorbitan type Span-20 to Span-80 are also used as AA compounds [111]. When used along with thermodynamic inhibitor (MeOH) or salts in the aqueous phase, they improve the inhibition efficiency [112, 113]. Increase in salinity increases ionic AA inhibition efficiency without disturbing emulsion stability [114]

Molecular simulation shows that AA could also promote hydrate growth [115] which could be used in hydrate based novel application such as natural gas storage and transportation, desalination, and other emerging applications.

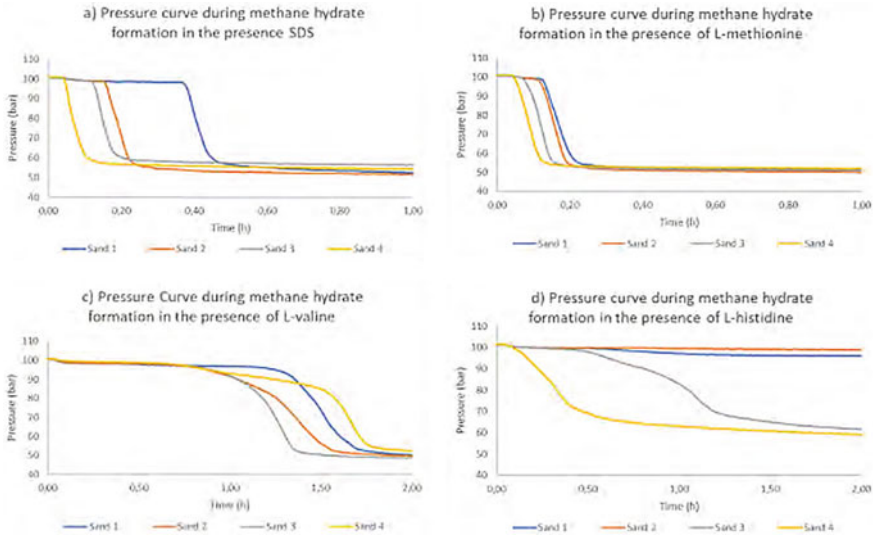

Fig. 9 Pressure variation during the isothermal experiments at 100 bar and 1°C comparing the methane hydrate formation kinetics for SDS and four selected amino acids (L-valine, L-methinonine, L- histidine, L-arginine) at given type of sand. Results indicate the hydrate formation rate increase as sand particle size increases in the presence of SDS and hydrophobic amino acids [104]

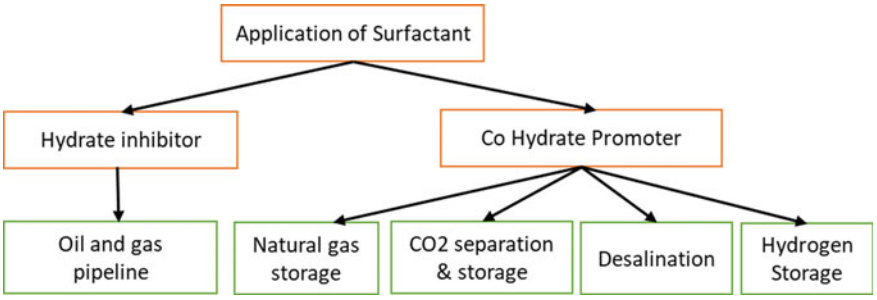

Fig. 10 Usage of Surfactant in different industries and applications

5.2 Natural Gas Storage and Transportation

Most crucial industrial development is in the field of natural gas (NG) storage and transportation, as gas hydrates offer additional benefits compared to traditional technologies like liquidified natural gas (LNG) and compressed natural gas (CNG). Methane gas hydrates offer high gas storage capacity in a solid-state, such that 170× methane gas per volume of hydrates (V/V) can be stored at moderate low-temperature (260–270 K) at atmospheric pressure due to self-preservation tendency shown by pure methane hydrates [116]. The storage and transport of NG in solid form

could be alternative to CNG [11]. In this regard, hydrate pelletization technology has been evaluated for the storage and transportation of NG [117, 118]. Stability was further improved in the presence of SDS [119] and maintained for 256 h with decomposition measured to be only 0.04% at 1 atm and 268.2 K. This ultrastability was caused due to different hydrate morphology in the presence of surfactant. Therefore, gas hydrates at subzero temperature show reduced gas leakage and offer added advantages compared to CNG and LNG transportation.

5.3 Hydrate Based Desalination and Produced Water Treatment

The feasibility of produced water and seawater treatment via gas hydrate formation was first demonstrated during the 1960 s [120]. This technique is based on the fundamental understanding of gas hydrates, that the chemical structure of gas hydrates includes only water and host molecules and excludes all salts and other impurities in unreacted water [121, 122]. Hydrate-based desalination has shown better efficiency compared to traditional desalination techniques, such as reverse osmosis and multistage distillation, at higher salinity levels up to 25%. Such high salinity in produced water has been reported in shale gas projects and CO_2 injection-based projects. Due to several reasons, including energy consumption, technology immaturity, low efficiency, hydrate-based technology was not used in desalination plants [123]. Recent studies using cyclopentane (CP) have shown promising results to be considered for desalination studies as CP forms hydrates with pure water under atmospheric pressure at 7 °C and is immiscible with pure water; therefore, it can be recycled after hydrate dissociation [124–126]. When water and CP come together, an emulsion is formed, and the use of CP is advantageous as it can be recovered at the end of dissociation. In the presence of promoter the hydrate formation rate, gas uptake, water recovery, and salt rejection improve. To make desalination more attractive, it is also suggested to combine cyclopentane with another guest molecule-based hydrate application, such as gas separation or gas capture to optimize energy consumption and improve the salt removal efficiency [127, 128]. Using surfactant with CP can bring more drawbacks than an advantages because its presence makes the hydrate former difficult to separate after dissociation [129]. Erfani et al. [130] studied the effect of 14 nonionic surfactants on the formation kinetics of CP hydrate and found that presence of surfactant decreased induction time and enhanced the hydrate formation rate. The surfactant, which generates an oil-in-water emulsion, performed better than water-in-oil emulsion. Lim et al. [24] found that SDS changes the CP hydrate morphology, which includes rectangular tree-like or fiber-like crystals, and no change in CP hydrate shell thickness was observed in the presence of surfactant [131]. To summarise based on results, key surfactants tested along with CP hydrate for desalination include LAE8EO, TritonX-100, NPE6EO, SDS, Dodecyltrimethylammonium bromide (DTB), Span-20, DDBSA (Dodecyl Benzene Sulfonic

Acid) and Tween 20 when used at a suitable concentration. Many surfactants, when added, modify CP hydrate morphology and physical properties. In the presence of surfactant CP solubility also enhances in water, and, hence, the removal of surfactant from the water at the end of dissociation is required as surfactants traditionally are toxic and not environmentally friendly. Use of bio-surfactants could be recommended in this application as they are biodegradable [37, 38, 132]

5.4 Hydrate Based CO_2 Separation, Capture and Storage

CO_2 separation, capture, and storage are important technology considerations to reduce greenhouse gas emission from industrial plants, including chemical, power, cement, etc. This technology includes pre and post-combustion CO2 capture. A pre-combustion gas mixture contains a CO_2/H_2 gas mixture, also known as fuel gas [14], while the post-combustion gas mixture includes CO_2/N_2 mixture known as flue gas. Hydrate-based CO_2 capture is proposed as a novel technique for CO_2 separation from fuel and flue gas mixtures [133–136]. The difference in CO_2 concentration in hydrate and in vapor phase acts as the main driver to separate CO_2 from the gas mixture during hydrate-based separation [15]. The key thermodynamic promoter used to achieve moderate operating conditions includes tetrahydrofuran (THF), tetrabutylammonium bromide (TBAB), tetra-n-butylammonium nitrate ($TBANO_3$), tetrabutylammonium fluoride (TBAF), and dodecyl trimethyl ammonium chloride (DTAC). Among these, THF is the most extensively used thermodynamic promoter for CO_2 separation and capture from the gas mixture.

Thermodynamic promoters are able to lower operational pressure or increase the temperature but do not have the influence of kinetics of the hydrate formation, which is essential for commercialization. Therefore, kinetic promoters including surfactants like SDS and SDBS (sodium dodecylbenzene sulfonate) have been used extensively along with thermodynamic promoters [137]. Among all tested surfactants, SDS was the most efficient. The CO_2–water system in the presence of SDS has shown lower induction time for CO_2 hydrate formation. CO_2 solubility increases in the presence of SDS due to a decrease in surface tension at the liquid-gas interface. Higher solubility causes faster nucleation and a further decrease in induction time [19, 62, 138] The growth rate is highest at 500–1000 ppm concentration, and higher concentration does not improve the growth rate and gas uptake [20]. In another study, it is suggested that SDS concentration has no effect on gas separation efficiency and only affects the rate of hydrate formation [139, 140]. When SDS is used with cyclopentane, no improvement in the kinetics of CO_2 hydrate formation are observed [136]. Presence of SDS during CH_4-CO_2 hydrate swapping can enhance CO_2 storage into methane hydrate reservoirs without disturbing geological formation [141] (Figure 11).

Fig. 11 Change in hydrate morphology in the presence of SDS 500 ppm in bulk water. Change in morphology is recorded before and after CO_2 injection into methane hydrate. Pictures also show the porous methane hydrate morphology. Methane hydate formed are porous in nature (Fig. 1). Figures 2–5 shows the morphgology change after CO_2 injection and 72 h after CO_2 injection [141]

5.5 Hydrate Based Hydrogen Storage

Application of hydrogen hydrates for stationary hydrogen storage has not taken off as hydrogen hydrates are formed at very high pressure (at the scale of GPa) at given ambient temperature. Research is focused on the use of kinetic and thermodynamic promoters and co-guest molecules to achieve moderate operating condition as well as faster formation kinetics [12, 142–144]. Some of the thermodynamic chemicals being tested repeatedly include TBAB, $TBANO_3$, THF, and CP [145–148]. Thermodynamic promoters occupy cages and reduces the hydrogen storage volume within hydrate. Apart from low hydrogen storage, low formation kinetics and risk of hydrogen diffusion through cages hinder adopting hydrate-based hydrogen storage methods at commercial scale [149–151]. Some researchers have tried to improve the hydrogen storage efficiency through different techniques [152–154]; however, there less attention is given to kinetics improvement, and very few studies have discussed the role of surfactant during hydrogen hydrate formation. SDS was found to be effective at the small concentration (5–500 ppm) during mixed hydrogen/propane hydrate formation studies, and two-stage hydrate growth was observed [155], a significant finding showing that micelles are unnecessary to impact hydrate formation (Fig. 12). Profile et al. [156] have invented a new technology with the help of aerosol OT surfactant(AOT), THF, and water and with the use of nanotechnology and isooctane.

5.6 Drawbacks of Surfactants

Surfactants have been studied extensively as kinetic promoters for hydrate formation; however, few studies have discussed the disadvantages of surfactants. The key disadvantage is that surfactants create foam even at low concentration (100–1000 ppm) during the degassing operation [157–159]. Due to foam formation, gas production rates can be very slow,which could be undesirable for industrial-scale applications. There are also concerns about surfactant biodegradability and their effect on environment [160]; therefore, current research is focused on environmentally friendly

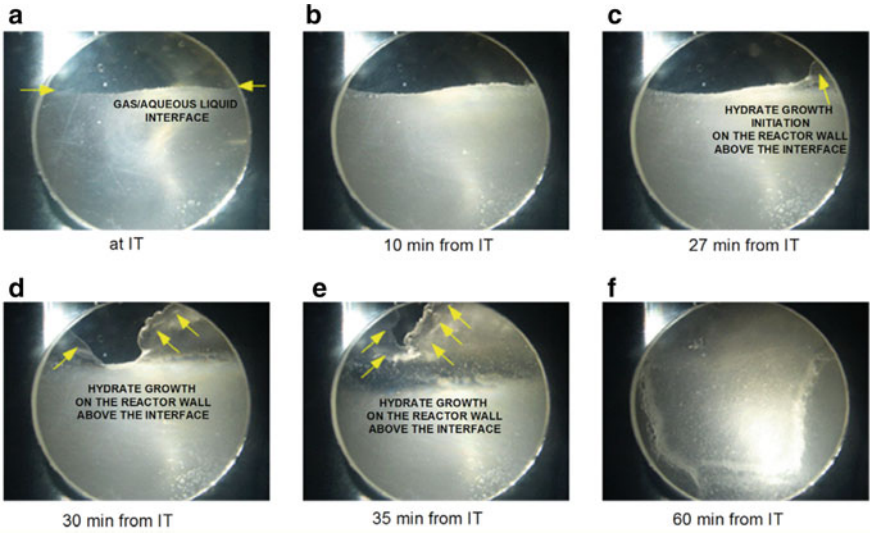

Fig. 12 Evidence of hydrate nucleation and growth at low concentration of SDS (25 ppm) within a mixed hydrogen−propane hydrate system performed at 274.2 K and 8.5 MPa in a stirred tank reactor. Reprinted from [156]

substitutes, such as amino acids [20] or new classes of biosurfactants [38] having similar kinetic promotion capabilities as anionic surfactants.

6 Computational Studies on the Role of Surfactant During Hydrate Formation

The first attempt to understand the blockage of pipelines due to gas hydrates has been by Hammerschmidt [6] in 1934. Among the first additives used to prevent the formation of gas hydrate included anti-freezing agents, such as methanol or ethylene glycol (EG). [161] Their effect in the solution resulted in a shift toward lower temperatures and higher pressures, due to a leftward change in the equilibrium phase boundary conditions. This came about because the hydrogen bonding between water and additive molecules affected the activity of water and the propensity to form hydrate cages [162], giving rise to the class of chemicals that are known as thermodynamic inhibitors. Such inhibitors have become commonplace in the oil and gas industry as preventative measures for gas hydrate formation and consequent pipeline blockage [163]. Conversely, there are chemicals that instead improve the formation behavior of hydrate by causing a shift of the phase boundary to the right, and they are thus known as thermodynamic promoters. These promoters are typically trapped in the hydrate cage along with the gas molecules, aiding in the stabilization of the hydrate crystalline structure at higher temperatures and/or lower pressures.

Thus, it is very valuable for oil and gas industries to be able to predict which additives and the correct amount that would be necessary to remove the risk of pipeline blockage resulting from gas hydrates. Hammerschmidt developed an early formula, considering the temperature that would suppress hydrate formation because of the inclusion of inhibiting chemicals, ΔT_H, as described in the work [6].

$$\Delta T_H = \frac{k_H w_{\text{add}}}{M_{\text{add}}(1 - w_{\text{add}})}$$

Here, k_H is a dimensionless constant that depends on the type of inhibitor, w_{add} is the mass fraction additive in aqueous solution, and M_{add} is its molecular weight. The equation is fairly simple and has relatively good accuracy, which makes it popular even to this day, despite more advanced models that have been developed since the 1950 s. However, because the accuracy of suppression temperature depends on estimation of the hydrate equilibrium temperature considering purity of samples, there is a higher chance of errors in calculation. In comparison, thermodynamic models primarily depend on the chemical potentials of each chemical in every phase being equal. Thus, thermodynamic models make it possible to include additives into calculations, insofar as parameters are provided for predicting their chemical potentials.

In the last decades, there has been a larger prevalence of first principles-based modeling since computational power has greatly increased over that time. This has made it possible to predict the properties of long chain molecules, typical of surfactants, ionic liquids, or amino acids, through methods like density functional theory (DFT). DFT typically has N_e^{2-3} scaling, where N_e is the number of electrons, which is why it has been a more recent endeavor for such molecules. More specifically, much research has been performed to understand the mechanisms of thermodynamic and kinetic hydrate inhibition (THI and KHI, respectively) arising from gas hydrate additives, both from experimental and computational aspects [164–167]. Very recently, Lee et al. were able to find synergistic effects when more than one inhibitor is utilized through a combination of both methods [168]. Statistical thermodynamics has gained much traction in the past years, since it can incorporate DFT-calculated properties into its calculation routine (e.g. the conductor-like screening model with real solvation, COSMO-RS) [169] to give information like reaction constant, activities, and Henry constants, to name a few [170–172].

Further implementation of first principles methods has been seen in the realm of artificial intelligence, as machine learning methods have been able to make predictions about properties using training sets with both experimental and computational data. The advantage of machine learning is that it can provide savings in computational time, given a large enough training set to give accurate results. Going into the future, as large scale operations will begin to implement gas hydrate production for various applications, computational fluid dynamics (CFD) and plant-scale simulations will benefit from incorporating these into a multi-scale approach, since each of these techniques span different time- and length-scales (see Fig. 13). Already,

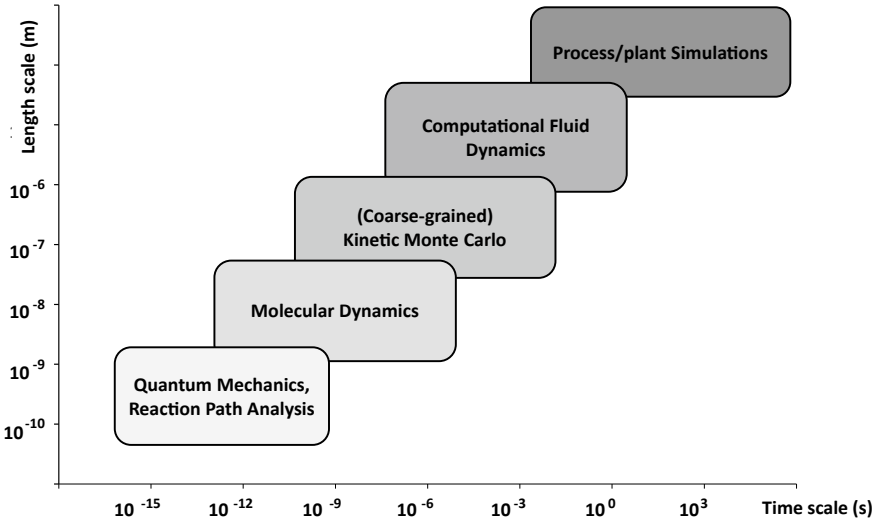

Fig. 13 How multi-scale modeling could link methods of different length- and time-scales

there has been some CFD simulations studying hydrate formation, and inclusion of additives will become increasingly prevalent.

Some key features of each of the methods above can be summarized in Table 2. In the following sections, the atomistic to micro-scale methods described above are presented with examples.

Table 2 Key usages and applications of the different computational methods

Method	Information gathered
Quantum mechanics	Relaxed structures of molecules/materials, interactions of small molecules, transition state searches
Molecular dynamics	Search for conformers, energy landscape of reactions, predict spectroscopic data
Kinetic monte carlo	Surface diffusion and growth, movement of defects and dislocations, viscoelasticity of crosslinking
Computational fluid dynamics	Movement of machinery, simulation of laminar/turbulent flows, heat transfer, aerodynamics, reacting flows and combustion
Process/plant simulations	Thermophysical properties, unit operation properties, chemical reactions/kinetics, environmenta/safety factors

6.1 Empirical Modelling—The Electrolyte Model

One particularly important application of models and property prediction, prior to the use of computationally-assisted models, pertains to equilibrium phase diagrams for gas hydrates and their additives, and the most common method of doing so—with good accuracy—has included estimated values for the activity of water as a function of additive. Dickens and Quinby-Hunt developed an electrolyte-based model [173] that could generate the equilibrium points for dissolved salts as additives, although it could be extended to ionic liquids and surfactants that can be viewed as separated charges [174], as has been proposed by Nashed et al. [175]. regarding ionic liquids as additives for methane hydrates. The electrolyte-based model is an adaptation of Pieroen's model [176], and has been utilized by many other works [177–180]. These models are based on classical thermodynamics, so assumptions, like negligible amount of gas in the hydrate and hydrate dissociation enthalpy (ΔH_{dis}) is constant over a small temperature range, are made, showing that additives decrease water activity (a_w). Thus, Nashed et al. made the following relationship between hydrate formation temperatures of pure water and the additive, T_w and T_{add}, respectively [175]:

$$\ln a_w = \frac{\Delta H_{\text{dis}}}{nR}\left(\frac{1}{T_w} - \frac{1}{T_{\text{add}}}\right)$$

where n is methane hydrate hydration number [181], and R is the universal gas constant. CSMGem software was used to calculate the water- methane hydrate dissociation temperature. The activity is also related to the change in freezing point due to additive, T_f and $T_{f,\text{ice}}$, for with and without additive, respectively, and the heat of fusion of ice:

$$\ln a_w = \frac{\Delta H_{\text{fus,ice}}}{R}\left(\frac{1}{T_{f,\text{ice}}} - \frac{1}{T_f}\right)$$

Combining the two equations above, one would be able to determine the effect of additives on the hydrate formation temperature.

In the work by Nashed et al. they were able to determine the phase boundaries of methane hydrates in the presence of 10 wt% ionic liquid solution experimentally, and found good agreement with the models above [175]. It was found that their impact caused a shift toward lower temperature and higher pressure, and a mean temperature reduction of 0.37–1.52 K was observed within their pressure range (5.1–11.1 MPa), depending on the type of ionic liquid used. More importantly, they drew relationships between the inhibition effect with chemical structure (e.g. cation/anion combinations and alkyl chain length), leading them to conclude that thermodynamic inhibitors are not involved in the formation of hydrate cages.

6.2 Quantum Mechanics

The presently most popular implementation of computational quantum mechanics is density functional theory (DFT), although others are used to lesser degrees, like configuration interaction, coupled cluster, and increasingly Møller-Plesset perturbation theory. One of the basic types of calculation that can be performed with DFT is the determination of the relaxed structure of a molecule and its corresponding energy. Using this information, one could, for example, use DFT (and, similarly, moleculdar dynamics) to determine the interaction energy, E_{int}, of a gas hydrate molecule with an inhibitor, given the gas hydrate energy, E_{GH}, the additive energy, E_{add}, and the energy of the interacting species, via:

$$E_{\text{int}} = E_{\text{GH+add}} - (E_{\text{GH}} + E_{\text{add}})$$

As an example, Lee et al. calculated the interaction energy between a cage and inhibitor molecule (amino acids and ionic liquids), and they found that the ionic liquid 1-butyl,3-methylimidazolium tertrafluoroborate had a greater probability of hydrate inhibition due to a stronger interaction energy compared to amino acid glycine [168]. This and many other binding energies can be compared in Table 3. Such relationships could be used in the reserve, to also determine improved hydrate formers, such as some surfactants (e.g. sodium dodecyl sulfate, SDS). Furthermore, these DFT calculations are used as a database to calculate larger systems, such as molecular dynamics simulations or statistical thermodynamics. Transition state theory is a method to determine the free energy barrier of reactions, of which the formation of gas hydrates could be applied, and DFT is commonly applied to it. However, molecular dynamics can be utilized the same way, as has been performed by Sicard et al. to understand how anti-agglomerants control methane transport with hydrates [106].

6.3 Molecular Dynamics

Molecular dynamics simulation is a very diverse and expanding field that can be utilized to calculate properties like surface tension, surfactant (reverse-) micellization in water/oil systems, bilayer and thin film formation, and looking just for such properties of SDS, there are already several sources [189–198]. Other studies of surfactant molecules have found a difference in the self-assembled structures due to changing conditions [199, 200].

More recently, a study by Choudhary et al. looked into the role of SDS (1 wt%) on methane hydrate formation in comparison with pure water [201], and it is one example of how simulations can be used to predict the influence of surfactants on gas hydrate growth behavior (Fig. 14). It was found that SDS tended to adsorb onto the hydrate surface because of its hydrophobic tail binding to openings in the cages

Table 3 Binding free energies calculated in literature from DFT or molecular dynamics simulations

Compound	sI Binding Free Energy [KJ/mol]	sII Binding Free Energy [KJ/mol]	Ref.	Note
CH_4	−32.51	−28.44	[182]	
CH_4	−30.42	−26.86	[183]	
C_2H_6	–	−39.45	[182]	
CO_2	–	−40.21	[182]	
N_2	−19.02	−20.05	[182]	
PVP 1-mer	6	–	[184]	
PVP 8-mer	−9	–	[184]	
PVP 16-mer	−21	–	[184]	
ChCl	−59.82, −118.21	−162.64, −155.37	[183]	
$ChTfn_2$	−12 to 132	−20 to 80	[185]	
ChOAc	28 to 88	8 to 118	[185]	
DB^3ACl	−1.2 to 68.6		[186]	*
PheAcA		−27.92	[187]	
NapAcA		−34.15	[187]	
PyrAcA		−53.75	[187]	
L-histidine	−47.20		[188]	**
Bicine	−48.91		[188]	**
L-serine	−44.73		[188]	**
Tricine	−29.47		[188]	**
Glycine	−47.88		[188]	**
Glycine	−52.46		[168]	
L-tyrosine	−63.68		[188]	**
L-threonine	−38.81		[188]	**
CAPB	−63.45		[188]	**
Betaine	−59.79		[188]	**
Proline	−48.41		[188]	**
Tryptophan	−44.43		[188]	**
$[BMIM][BF_4]$	−393.46		[168]	

PVP = polyvinylpyrrolidone, ChCl = choline chloride, $ChTfn_2$ = choline bistriflamide, ChOAc = choline acetate, DB^3ACl = n-dodecyl-tri(n-butyl)-ammonium chloride, PheAcA = 1-phenylacetic acid, NapAcA = 2-napthylacetic acid, PyrAcA = 1-pyreneacetic acid, CAPB = cocamidopropyl betaine, $[BMIM][BF_4]$ = 1-butyl-3-methylimidazolium tetrafluoroborate. *Molecular dynamics simulation with mixed hydrate sizes. **Averaged over interaction sites, binding with water molecule

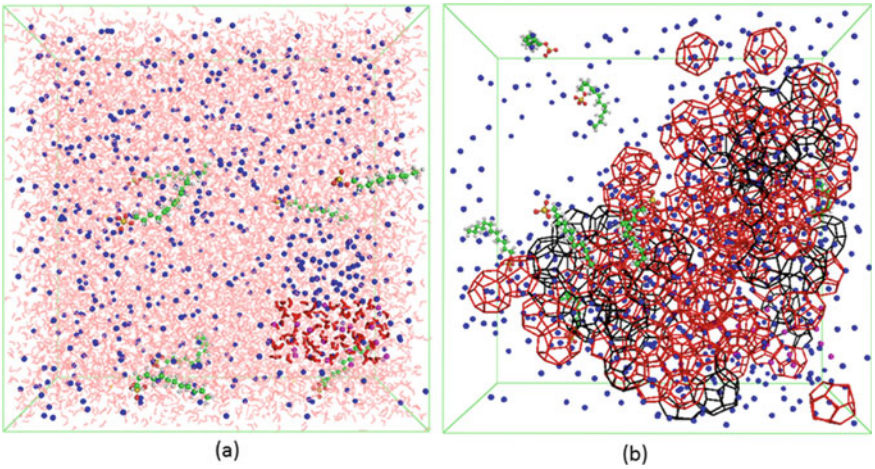

Fig. 14 Molecular dynamics simulation of **a** a mixture of methane, water, and 1% SDS and **b** a snapshot after 1 μs at 270 K and 100 bar, showing significant 5^{12} (black cage) and $5^{12}6^2$ (red cage) hydrate formation (water molecules hidden in **b**). Key for dots: liquid water (light red), seed water (dark red), methane (blue), methane of seed (magenta), carbon of hydrophobic SDS tail (green), sulfur (yellow), hydrogen (white), and oxygen of SDS (red). Reprinted from [201]

of growing hydrates, which they report caused it to stabilize the nascent nuclei. This was expected to reduce the surface energy and thus also the nucleation barrier and induction time. They believe that these adsorbed surfactant molecules might change the morphology of the hydrate as it grows of larger length and time scales. The porosity could increase the mass transfer of guest molecule, leading to improved growth kinetics of the gas hydrate.

Another molecular dynamics study of SDS with methane hydrates found that micellization of the molecule was not required during the formation of gas hydrates [50].

Great interest has been invested in understanding formation kinetics using molecular simulations [202]. One such study by Walsh et al. [203] found that during the nucleation process the interaction of guest molecules with the faces and surfaces of partial hydrate cages led to the formation of the full gas hydrate. This and the many other studies have been able to improve the understanding of how additives may affect hydrate formation, such the simulations of CO_2 and CH_4 gas hydrates [204] leading to the further study on the impact of tetrahydrofuran on their formation [205].

In another important study, Carver et al. [206], using Monte Carlo simulations, found that the effect of PVP as an inhibitor depended on pendant hydrogens on the hydrate surface being available as adsorption sites, since PVP would lie along the surface and block these sites. Furthermore, Bui et al. studied how anti-agglomerants could either enhance or impair hydrate formation [107]. Similarly, other groups studied how sodium chloride might influence the adsorption behavior

of anti-agglomerants [207, 208], surfactants like SDS, and hydrocarbons [209]. In another study by Bui et al. [105], they were able to reproduce micromechanical force experiments using equilibrium molecular dynamics.

Large systems have also been utilized with stochastic models like Kinetic Monte Carlo simulations. Understandings of agglomeration [210] and surface diffusion [108] behaviors of hydrates due to surfactacts have been particularly impacted by such Big Picture approaches.

6.4 Continuum Solvation Model

As mentioned above, conductor-like screening model with real solvation (COSMO-RS) can be employed to calculate many thermodynamic properties, in an approach different from molecular dynamics [169]. Taking advantage of the large database and promising nature (low vapor pressure, tunability, and bifunctionality) of ionic liquids, Bavoh et al. screened potential candidates for gas hydrate inhibition, rather than relying on trial and error, which are time intensive [211].

Athough group contribution (GC) methods, such as UNIQUAC Functional-group Activity Coefficients (UNIFAC), are commonplace and reliable for thermodynamic property prediction, they are lacking in accuracy when the groups are less studied experimentally or have long chains, such as in the case of ionic liquids. Thus, using a tool which is based on first principles becomes more attractive, considering its high accuracy [212]. It is already commonly used in pharmaceutical research and chemical engineering [213–215].

Bavoh et al. presented COSMO-RS as a novel prescreening tool for ionic liquid-based hydrate mitigation by correlating their calculated hydrogen bonding energies (E_{HB}) with suppression temperature, ΔT_H, in comparison with induction time studies. Their work was able to describe the factors that impact the E_{HB} of ionic liquids in terms of hydrogen bond donors and acceptors, through the use of sigma profiles and potentials that are generated with COSMO-RS.

Similar studies could be performed with a focus, for example, on screening of surfactant molecules that can aid in gas hydrate formation, since the work by Bavoh et al. is one of the first to apply COSMO-RS calculations for gas hydrate applications, and it was limited to ionic liquids. There are still many ionic liquids that are not included in the database of commercially available software, which would also expand the scope of ionic liquids screening.

6.5 Machine Learning

An example of the application of machine learning for studying gas hydrates can be found in the work done by Xia et al. [216]. They incorporated a fusion modeling method that could be used to predict CO_2 solubility in hydrates as related to nine

ionic liquids. Using data collected from literature, they divided them into three sets, some for training, some for validation, and the rest for testing. With the training set, they were able to incorporate the back propagation neural network, support vector machine, and extreme learning machine. From these, three sub-models with the best performance were chosen according to the validation set. Afterwards, linear fusion models were included via the minimum square error and information entropy methods. Lastly, the prediction performance of these last sets of models was evaluated with the test set, which found that their linear fusion model was the best performing, with the information entropy method having better predictions. However, they do clarify that although their predictions worked well, they were not guaranteed to work on ionic liquids outside of the nine they tested, but it is something that is amenable to future expansion and has tremendous time savings compared to the alternatives, and it could rival COSMO-RS in the prediction of thermodynamic properties.

7 Closing Remarks and Future Prospects

In this chapter, an introduction into surfactant-based hydrate promotion studies was provided. Key areas that were touched include a summary of the theories proposed and how they have been implemented computationally, as well as discussions on surfactant-supported promoters. Based on the discussion, the following remarks can be added as the conclusion and future prospects

- Many theories are suggested to explain the role of surfactants during hydrate promotion. Micellar and capillary-based theories are the two most prominent ones. The capillary effect in particular plays a critical role.
- The molecular structure of a surfactant controls the hydrate formation efficiency, and surfactants with optimal structures would outperform the rest of the surfactants. Key factors that play a part in enhancing the efficiency include the ionic strength and chain length.
- Surfactants also play a key role along with other co-promoters since surfactants affect formation in different ways, including stabilization, kinetic improvements, etc., at a suitable concentration.
- The success of hydrate-based industrial applications depends on optimal use of surfactants along with other promoters and mechanical techniques.
- Use of biosurfactants is gaining attention due to their biodegradability. More research is required regarding the use of biosurfactant in desalination.
- Use of surfactants to improve hydrate formation kinetics is not well discussed in emerging technologies, including hydrogen storage, cold storage, etc.
- Computational modeling has given a large number of insights into the understanding experimental observations, and they have assisted in smart design selection of surfactants and other additives.

- Multi-scale modeling from quantum-scale to plant-scale will prove to be a major breakthrough in hydrate formation and storage, since it would be able to predict the appropriate surfactants and physical conditions that make the applications feasible and efficient.

References

1. Sloan ED, Koh CA, Koh C (2007) *Clathrate hydrates of natural gases*, 3rd edn, CRC Press
2. Koh CA (2002) Towards a fundamental understanding of natural gas hydrates. Chem Soc Rev 31:157–167
3. Makogon YF (2010) Natural gas hydrates—a promising source of energy. J Nat Gas Sci Eng
4. Boswell R, Collett TS (2011) Current perspectives on gas hydrate resources. Energy Environ Sci 4:1206–1215
5. Shina K, Kumarb R, Udachina KA, Alavia S, Ripmeester JA (2012) Ammonia clathrate hydrates as new solid phases for Titan, Enceladus, andother planetary systems. Proc Natl Acad Sci USA 109:14785–14790
6. Hammerschmidt EG (1934) Formation of gas hydrates in natural gas transmission lines. Ind Eng Chem 26:851–855
7. Jamaluddin AKM, Kalogerakis N, Bishnoi PR (1991) Hydrate plugging problems in undersea natural gas pipelines under shutdown conditions. J Pet Sci Eng 5:323–335
8. Kelland MA (2006) History of the development of low dosage hydrate inhibitors. Energy Fuels 20:825–847
9. Chua PC, Kelland MA (2018) Study of the gas hydrate antiagglomerant performance of a series of mono-and bis-amine oxides: dual antiagglomerant and kinetic hydrate inhibition behavior. Energy Fuels 32:1674–1684
10. Englezos P, Lee JD (2005) Gas hydrates: a cleaner source of energy and opportunity for innovative technologies. Korean J Chem Eng 22:671–681
11. Veluswamy HP, Kumar A, Seo Y, Lee JD, Linga P (2018) A review of solidified natural gas (SNG) technology for gas storage via clathrate hydrates. Appl Energy 216:262–282
12. Veluswamy HP, Kumar R, Linga P (2014) Hydrogen storage in clathrate hydrates: current state of the art and future directions. Appl Energy 122:112–132
13. Dashti H, Yew LZ, Lou X Recent advances in gas hydrate-based CO2 capture.pdf
14. Babu P, Linga P, Kumar R, Englezos P (2015) A review of the hydrate based gas separation (HBGS) process for carbon dioxide pre-combustion capture. Energy 85:261–279
15. Li A, Wang J, Bao B (2019) High-efficiency CO_2 capture and separation based on hydrate technology: a review. Greenh Gases Sci Technol 9:175–193
16. Babu P, Nambiar A, He T, Karimi IA, Lee JD, Englezos P, Linga P (2018) A review of clathrate hydrate based desalination to strengthen energy-water nexus. ACS Sustain Chem Eng 6:8093–8107
17. Gayet P, Dicharry C, Marion G, Graciaa A, Lachaise J, Nesterov A (2005) Experimental determination of methane hydrate dissociation curve up to 55 MPa by using a small amount of surfactant as hydrate promoter 60:5751–5758
18. Kalogerakis N, Jamaluddin AKM, Dholabhai PD, Bishnoi PR (1993) Effect of surfactants on hydrate formation kinetics. In: Proceedings of the proceedings of the 1993 spe international symposium on oilfield chemistry, Society of Petroleum Engineers 1:375–383
19. Kumar A, Bhattacharjee G, Kulkarni BD, Kumar R (2015) Role of surfactants in promoting gas hydrate formation. Ind Eng Chem Res 54:12217–12232
20. Pandey JS, Daas YJ, Solms N (2020) Von screening of amino acids and surfactant as hydrate promoter for CO_2 capture from flue gas

21. Kvamme B, Selvåg J, Saeidi N, Kuznetsova T (2018) Methanol as a hydrate inhibitor and hydrate activator. Phys Chem Chem Phys 20:21968–21987
22. Linga P, Clarke MA (2017) A review of reactor designs and materials employed for increasing the rate of gas hydrate formation. Energy Fuels 31:1–13
23. Kumar A, Sakpal T, Linga P, Kumar R (2015) Enhanced carbon dioxide hydrate formation kinetics in a fixed bed reactor filled with metallic packing. Chem Eng Sci 122:78–85
24. Lim YA, Babu P, Kumar R, Linga P (2013) Morphology of carbon dioxide-hydrogen-cyclopentane hydrates with or without sodium dodecyl sulfate. Cryst Growth Des 13:2047–2059
25. Yagasaki T, Matsumoto M, Andoh Y, Okazaki S, Tanaka H (2014) Effect of bubble formation on the dissociation of methane hydrate in water: A molecular dynamics study. J Phys Chem B 118:1900–1906
26. Zhang JS, Lee S, Lee JW (2007) Kinetics of methane hydrate formation from sds solution, pp 6353–6359
27. Zhang J, Lee JW (2009) Effect of sodium dodecyl sulfate on the supercooling point of ice and clathrate hydrates. Energy Fuels 23:3045–3047
28. Zhong Y, Rogers RE (2000) Surfactant effects on gas hydrate formation. Chem Eng Sci 55:4175–4187
29. World THE, Surface OF The world of surface science *, pp 14–24
30. Fuhrhop JH, Koning J (1994) *Membranes and molecular assemblies*, Monographs in supramolecular chemistry, The Royal Society of Chemistry, ISBN 978-0-85186-732-8
31. He Y, Sun M-T, Chen C, Zhang G-D, Chao K, Lin Y, Wang F (2019) Surfactant-based promotion to gas hydrate formation for energy storage. J Mater Chem A 7:21634–21661
32. Karaaslan U, Parlaktuna M (2002) Promotion effect of polymers and surfactants on hydrate formation rate. Energy Fuels 16:1413–1416
33. Karaaslan U, Parlaktuna M (2000) Surfactants as hydrate promoters? Energy Fuels 14:1103–1107
34. Okutani K, Kuwabara Y, Mori YH (2008) Surfactant effects on hydrate formation in an unstirred gas / liquid system : an experimental study using methane and sodium alkyl sulfates 63:183–194
35. Kumar A, Sakpal T, Linga P, Kumar R (2013) Influence of contact medium and surfactants on carbon dioxide clathrate hydrate kinetics. Fuel 105:664–671
36. Veluswamy HP, Ang WJ, Zhao D, Linga P (2015) In fl uence of cationic and non-ionic surfactants on the kinetics of mixed hydrogen / tetrahydrofuran hydrates. Chem Eng Sci 132:186–199
37. Rogers RE, Kothapalli C, Lee MS, Woolsey JR (2008) Catalysis of Gas Hydrates by Biosurfactants in Seawater-Saturated Sand/Clay. Can J Chem Eng 81:973–980
38. Arora A, Cameotra SS, Kumar R, Balomajumder C, Singh AK, Santhakumari B, Kumar P, Laik S (2016) Biosurfactant as a promoter of methane hydrate formation: thermodynamic and kinetic studies. Sci Rep 6:1–13
39. Rogers R, Zhang G, Dearman J, Woods C (2007) Investigations into surfactant/gas hydrate relationship. J Pet Sci Eng 56:82–88
40. Barakat Y, Fortney LN, Schechter RS, Wade WH, Yiv SH, Graciaa A (1983) Criteria for structuring surfactants to maximize solubilization of oil and water. II. Alkyl benzene sodium sulfonates. J Colloid Interface Sci 92:561–574
41. Kunieda H, Shinoda K (1982) Correlation between critical solution phenomena and ultralow interfacial tensions in a surfactant/water/oil system. Chem Soc Japan 55:1777–1781
42. Daimaru T, Yamasaki A, Yanagisawa Y (2007) Effect of surfactant carbon chain length on hydrate formation kinetics. J Pet Sci Eng 56:89–96
43. Dicharry C, Diaz J, Torré JP, Ricaurte M (2016) Influence of the carbon chain length of a sulfate-based surfactant on the formation of CO_2, CH_4 and CO_2–CH_4 gas hydrates. Chem Eng Sci 152:736–745
44. Roy S, Mehra A, Bhowmick D (1997) Prediction of solubility of nonpola—gases in micellar solutions of ionic surfactants. J Colloid Interface Sci 196:53–61

45. Luo H, Sun CY, Peng BZ, Chen GJ (2006) Solubility of ethylene in aqueous solution of sodium dodecyl sulfate at ambient temperature and near the hydrate formation region. J Colloid Interface Sci 298:952–956
46. Peng BZ, Chen GJ, Luo H, Sun CY (2006) Solubility measurement of methane in aqueous solution of sodium dodecyl sulfate at ambient temperature and near hydrate conditions. J Colloid Interface Sci 304:558–561
47. Pandey JS, Daas YJ, Solms N (2019) Von insights into kinetics of methane hydrate formation in the presence of surfactants
48. Di Profio P, Arca S, Germani R, Savelli G (2005) Surfactant promoting effects on clathrate hydrate formation: Are micelles really involved? Chem Eng Sci 60:4141–4145
49. Zhang JS, Lee S, Lee JW (2007) Does SDS micellize under methane hydrate-forming conditions below the normal Krafft point? J Colloid Interface Sci 315:313–318
50. Albertí M, Costantini A, Laganá A, Pirani F (2012) Are micelles needed to form methane hydrates in sodium dodecyl sulfate solutions? J Phys Chem B 116:4220–4227
51. Kobayashi I, Ito Y, Mori YH (2001) Microscopic observations of clathrate-hydrate films formed at liquid/liquid interfaces. I. Morphology of hydrate films. Chem Eng Sci 56:4331–4338
52. Watanabe K, Imai S, Mori YH (2005) Surfactant effects on hydrate formation in an unstirred gas/liquid system: An experimental study using HFC-32 and sodium dodecyl sulfate. Chem Eng Sci 60:4846–4857
53. Yoslim J, Linga P, Englezos P (2010) Enhanced growth of methane—propane clathrate hydrate crystals with sodium dodecyl sulfate, sodium tetradecyl sulfate, and sodium hexadecyl sulfate surfactants. J Cryst Growth 313:68–80
54. Karanjkar PU, Lee JW, Morris JF (2012) Surfactant effects on hydrate crystallization at the water-oil interface: hollow-conical crystals. Cryst Growth Des 12:3817–3824
55. Tajima H, Kiyono F, Yamasaki A (2010) Direct observation of the effect of sodium dodecyl sulfate (SDS) on the gas hydrate formation process in a static mixer. Energy Fuels 24:432–438
56. Mitarai M, Kishimoto M, Suh D, Ohmura R (2015) Surfactant effects on the crystal growth of clathrate hydrate at the interface of water and hydrophobic-guest liquid. Cryst Growth Des 15:812–821
57. Hayama H, Mitarai M, Mori H, Verrett J, Servio P, Ohmura R (2016) Surfactant Effects on Crystal Growth Dynamics and Crystal Morphology of Methane Hydrate Formed at Gas/Liquid Interface. Cryst Growth Des 16:6084–6088
58. Hayama H, Mitarai M, Mori H, Ohmura R (2016) Methane hydrate crystal growth at the gas/liquid interface in the presence of sodium dodecyl sulfate. Procedia Eng 148:339–345
59. Wang F, Wang L, Wang C, Guo G, Liu G, Luo S, Guo R (2015) Direction controlled methane hydrate growth. Cryst Growth Des 15:5112–5117
60. Wang F, Jia ZZ, Luo SJ, Fu SF, Wang L, Shi XS, Wang CS, Guo RB (2015) Effects of different anionic surfactants on methane hydrate formation. Chem Eng Sci 137:896–903
61. Botimer JD, Dunn-Rankin D, Taborek P (2016) Evidence for immobile transitional state of water in methane clathrate hydrates grown from surfactant solutions. Chem Eng Sci 142:89–96
62. Molokitina NS, Nesterov AN, Podenko LS, Reshetnikov AM (2019) Carbon dioxide hydrate formation with SDS: Further insights into mechanism of gas hydrate growth in the presence of surfactant. Fuel 235:1400–1411
63. Ando N, Kuwabara Y, Mori YH (2012) Surfactant effects on hydrate formation in an unstirred gas/liquid system: an experimental study using methane and micelle-forming surfactants. Chem Eng Sci 73:79–85
64. Wang F, Liu GQ, Meng HL, Guo G, Luo SJ, Guo RB (2016) Improved methane hydrate formation and dissociation with nanosphere-based fixed surfactants as promoters. ACS Sustain Chem Eng 4:2107–2113
65. Daniel-David D, Guerton F, Dicharry C, Torré JP, Broseta D (2015) Hydrate growth at the interface between water and pure or mixed CO2/CH4 gases: Influence of pressure, temperature, gas composition and water-soluble surfactants. Chem Eng Sci 132:118–127

66. Zhang JS, Lo C, Somasundaran P, Lu S, Couzis A, Lee JW (2008) Adsorption of sodium dodecyl sulfate at THF hydrate/liquid interface. J Phys Chem C 112:12381–12385
67. Zhang JS, Lo C, Somasundaran P, Lee JW (2010) Competitive adsorption between SDS and carbonate on tetrahydrofuran hydrates. J Colloid Interface Sci 341:286–288
68. Lo C, Zhang JS, Couzis A, Somasundaran P, Lee JW (2010) Adsorption of cationic and anionic surfactants on cyclopentane hydrates. J Phys Chem C 114:13385–13389
69. Schramm LL, Stasiuk EN, Marangoni DG (2003) Surfactants and their applications. Annu Rep Prog Chem Sect C 99:3–48
70. Scamehorn JF, Schechter RS, Wade WH (1982) Adsorption of surfactants on mineral oxide surfaces from aqueous solutions. I: Isomerically pure anionic surfactants. J Colloid Interface Sci 85:463–478
71. Somasundaran P, Fuerstenau DW (1966) Mechanisms of alkyl sulfonate adsorption at the alumina-water interface. J Phys Chem 70:90–96
72. Zerpa LE, Salager JL, Koh CA, Sloan ED, Sum AK (2011) Surface chemistry and gas hydrates in flow assurance. Ind Eng Chem Res 50:188–197
73. Song JH, Couzis A, Lee JW (2010) Investigation of macroscopic interfacial dynamics between clathrate hydrates and surfactant solutions. Langmuir 26:18119–18124
74. Torré JP, Dicharry C, Ricaurte M, Daniel-David D, Broseta D (2011) CO2 capture by hydrate formation in quiescent conditions: in search of efficient kinetic additives. Energy Procedia 4:621–628
75. Torre J, Ricaurte M, Dicharry C, Broseta D (2012) CO2 enclathration in the presence of water-soluble hydrate promoters: Hydrate phase equilibria and kinetic studies in quiescent conditions. Chem Eng Sci 82:1–13
76. Li X, Chen C, Chen Y, Li Y, Li H (2015) Kinetics of methane clathrate hydrate formation in water-in-oil emulsion. Energy Fuels 29:2277–2288
77. Dalmazzone D, Hamed N, Dalmazzone C (2009) DSC measurements and modelling of the kinetics of methane hydrate formation in water-in-oil emulsion T / K 64:2020–2026
78. Mu L, Li S, Ma QL, Zhang K, Sun CY, Chen GJ, Liu B, Yang LY (2014) Experimental and modeling investigation of kinetics of methane gas hydrate formation in water-in-oil emulsion. Fluid Phase Equilib 362:28–34
79. Xiang CS, Peng BZ, Liu H, Sun CY, Chen GJ, Sun BJ (2013) Hydrate formation/dissociation in (Natural Gas + Water + Diesel Oil) emulsion systems. Energies 6:1009–1022
80. Lv X, Shi B, Zhou S, Peng H, Lei Y, Yu P (2018) Study on the growth rate of natural gas hydrate in water-in-oil emulsion system using a high-pressure flow loop. RSC Adv 8:36484–36492
81. Ding K, Zhong DL, Lu YY, Le Wang J (2015) Enhanced precombustion capture of carbon dioxide by gas hydrate formation in Water-In-Oil emulsions. Energy Fuels 29:2971–2978
82. A water droplet size distribution dependent modeling of hydrate formation in water/oil emulsion
83. Yegya Raman AK, Venkataramani D, Bhagwat S, Martin T, Clark PE, Aichele CP (2016) Emulsion stability of surfactant and solid stabilized water-in-oil emulsions after hydrate formation and dissociation. Colloids Surf A Physicochem Eng Asp 506:607–621
84. Nashed O, Partoon B, Lal B, Sabil KM, Shariff AM (2018) Review the impact of nanoparticles on the thermodynamics and kinetics of gas hydrate formation. J Nat Gas Sci Eng 55:452–465
85. Said S, Govindaraj V, Herri JM, Ouabbas Y, Khodja M, Belloum M, Sangwai JS, Nagarajan R (2016) A study on the influence of nanofluids on gas hydrate formation kinetics and their potential: application to the CO_2 capture process. J Nat Gas Sci Eng 32:95–108
86. Arjang S, Manteghian M, Mohammadi A (2013) Effect of synthesized silver nanoparticles in promoting methane hydrate formation at 4.7 MPa and 5.7MPa. Chem Eng Res Des 91:1050–1054
87. Rahmati-Abkenar M, Manteghian M, Pahlavanzadeh H (2017) Experimental and theoretical investigation of methane hydrate induction time in the presence of triangular silver nanoparticles. Chem Eng Res Des 120:325–332
88. Rahmati-Abkenar M, Manteghian M, Pahlavanzadeh H (2017) Nucleation of ethane hydrate in water containing silver nanoparticles. Mater Des 126:190–196

89. Kakati H, Mandal A, Laik S (2016) Promoting effect of Al2O3/ZnO-based nanofluids stabilized by SDS surfactant on CH4+C2H6+C3H8 hydrate formation. J Ind Eng Chem 35:357–368
90. Aliabadi M, Rasoolzadeh A, Esmaeilzadeh F, Alamdari AM (2015) Experimental study of using CuO nanoparticles as a methane hydrate promoter. J Nat Gas Sci Eng 27:1518–1522
91. Najibi H, Mirzaee Shayegan M, Heidary H (2015) Experimental investigation of methane hydrate formation in the presence of copper oxide nanoparticles and SDS. J Nat Gas Sci Eng 23:315–323
92. Kumar A, Kushwaha OS, Rangsunvigit P, Linga P, Kumar R (2016) Effect of additives on formation and decomposition kinetics of methane clathrate hydrates: application in energy storage and transportation. Can J Chem Eng 94:2160–2167
93. Veluswamy HP, Kumar S, Kumar R, Rangsunvigit P, Linga P (2016) Enhanced clathrate hydrate formation kinetics at near ambient temperatures and moderate pressures: application to natural gas storage. Fuel 182:907–919
94. Mech D, Gupta P, Sangwai JS (2016) Kinetics of methane hydrate formation in an aqueous solution of thermodynamic promoters (THF and TBAB) with and without kinetic promoter (SDS). J Nat Gas Sci Eng 35:1519–1534
95. Kakati H, Mandal A, Laik S (2016) Effect of SDS/THF on thermodynamic and kinetic properties of formation of hydrate from a mixture of gases (CH4+C2H6+C3H8) for storing gas as hydrate. J Energy Chem 25:409–417
96. Pan Z, Liu Z, Zhang Z, Shang L, Ma S (2018) Effect of silica sand size and saturation on methane hydrate formation in the presence of SDS. J Nat Gas Sci Eng 56:266–280
97. Østergaard KK, Anderson R, Llamedo M, Tohidi B (2002) Hydrate phase equilibria in porous media: Effect of pore size and salinity. Terra Nov 14:307–312
98. Moroi Y, Matuura R (1988) Thermodynamics of solubilization into surfactant micelles: effect of hydrophobicity of both solubilizate and surfactant molecules. J Colloid Interface Sci 125:456–462
99. Mandal A, Laik S (2008) Effect of the promoter on gas hydrate formation and dissociation. Energy Fuels 22:2527–2532
100. Nashed O, Partoon B, Lal B, Sabil KM, Shariff AM (2019) Investigation of functionalized carbon nanotubes' performance on carbon dioxide hydrate formation. Energy 174:602–610
101. Choi JW, Chung JT, Kang YT (2014) CO2 hydrate formation at atmospheric pressure using high efficiency absorbent and surfactants. Energy 78:869–876
102. Yang M, Song Y, Jiang L, Zhao Y, Ruan X, Zhang Y, Wang S (2014) Hydrate-based technology for CO2 capture from fossil fuel power plants. Appl Energy 116:26–40
103. Liu Z, Pan Z, Zhang Z, Liu P, Shang L, Li B (2018) Effect of porous media and sodium dodecyl sulphate complex system on methane hydrate formation. Energy Fuels 32:5736–5749
104. Pandey JS, Daas YJ, von Solms N (2020) Methane hydrate formation, storage and dissociation behavior in unconsolidated sediments in the presence of environment-friendly promoters
105. Bui T, Phan A, Monteiro D, Lan Q, Ceglio M, Acosta E, Krishnamurthy P, Striolo A (2017) Evidence of structure-performance relation for surfactants used as antiagglomerants for hydrate management. Langmuir 33:2263–2274
106. Sicard F, Bui T, Monteiro D, Lan Q, Ceglio M, Burress C, Striolo A (2018) Emergent properties of antiagglomerant films control methane transport: implications for hydrate management. Langmuir 34:9701–9710
107. Bui T, Sicard F, Monteiro D, Lan Q, Ceglio M, Burress C, Striolo A (2018) Antiagglomerants affect gas hydrate growth. J Phys Chem Lett 9:3491–3496
108. Phan A, Bui T, Acosta E, Krishnamurthy P, Striolo A (2016) Molecular mechanisms responsible for hydrate anti-agglomerant performance. Phys Chem Chem Phys 18:24859–24871
109. Tokiwa Y, Sakamoto H, Takiue T, Aratono M, Matsubara H (2015) Effect of alkane chain length and counterion on the freezing transition of cationic surfactant adsorbed film at alkane mixture—water interfaces. J Phys Chem B 119:6235–6241
110. Lei Q, Bain CD (2004) Surfactant-induced surface freezing at the alkane-water interface. Phys Rev Lett 92:2–5

111. Huo Z, Freer E, Lamar M, Sannigrahi B, Knauss DM, Sloan ED (2001) Hydrate plug prevention by anti-agglomeration. Chem Eng Sci 56:4979–4991
112. York JD, Firoozabadi A (2009) Effect of brine on hydrate antiagglomeration. Energy Fuels 23:2937–2946
113. York JD, Firoozabadi A (2008) Alcohol cosurfactants in hydrate antiagglomeration. J Phys Chem B 112:10455–10465
114. Aman ZM, Haber A, Ling NNA, Thornton A, Johns ML, May EF (2015) Effect of brine salinity on the stability of hydrate-in-oil dispersions and water-in-oil emulsions. Energy Fuels 29:7948–7955
115. Striolo A, Phan A, Walsh MR (2019) Molecular properties of interfaces relevant for clathrate hydrate agglomeration. Curr Opin Chem Eng 25:57–66
116. Stern LA, Circone S, Kirby SH, Durham WB (2001) Anomalous preservation of pure methane hydrate at 1 atm. J Phys Chem B 105:1756–1762
117. Kang HJ, Yang Y, Ki MS, Shin MS, Choi J, Cha JH, Lee D (2016) A concept study for cost effective NGH mid-stream supply chain establishing strategies. Ocean Eng 113:162–173
118. Rehder G, Eckl R, Elfgen M, Falenty A, Hamann R, Kähler N, Kuhs WF, Osterkamp H, Windmeier C (2012) Methane hydrate pellet transport using the self-preservation effect: a techno-economic analysis. Energies 5:2499–2523
119. Zhang G, Rogers RE (2008) Ultra-stability of gas hydrates at 1 atm and 268.2 K. Chem Eng Sci 63:2066–2074
120. Subramani A, Jacangelo JG (2015) Emerging desalination technologies for water treatment: a critical review. Water Res 75:164–187
121. Kang KC, Linga P, Park KN, Choi SJ, Lee JD (2014) Seawater desalination by gas hydrate process and removal characteristics of dissolved ions (Na+, K+, Mg2+, Ca2+, B3+, Cl−, SO42−). Desalination 353:84–90
122. Park KN, Hong SY, Lee JW, Kang KC, Lee YC, Ha MG, Lee JD (2011) A new apparatus for seawater desalination by gas hydrate process and removal characteristics of dissolved minerals (Na+, Mg2+, Ca2+, K+, B3+). Desalination 274 91–96
123. He T, Nair SK, Babu P, Linga P, Karimi IA (2018) A novel conceptual design of hydrate based desalination (HyDesal) process by utilizing LNG cold energy. Appl Energy 222:13–24
124. Li F, Chen Z, Dong H, Shi C, Wang B, Yang L, Ling Z (2018) Promotion effect of graphite on cyclopentane hydrate based desalination. Desalination 445:197–203
125. Hong S, Moon S, Lee Y, Lee S, Park Y (2019) Investigation of thermodynamic and kinetic effects of cyclopentane derivatives on CO2 hydrates for potential application to seawater desalination. Chem Eng J 363:99–106
126. McAuliffe C (1966) Solubility in water of paraffin, cycloparaffin, olefin, acetylene, cycloolefin, and aromatic hydrocarbons. J Phys Chem 70:1267–1275
127. Herslund PJ, Thomsen K, Abildskov J, Von Solms N (2014) Modelling of cyclopentane promoted gas hydrate systems for carbon dioxide capture processes. Fluid Phase Equilib 375:89–103
128. Herri JM, Bouchemoua A, Kwaterski M, Brântuas P, Galfré A, Bouillot B, Douzet J, Ouabbas Y, Cameirao A (2014) Amélioration de la sélectivité du captage du CO_2 dans les semi-clathrates hydrates en utilisant les ammoniums quaternaires comme promoteurs thermodynamiques. Oil Gas Sci Technol 69:947–968
129. Ho-Van S, Bouillot B, Douzet J, Babakhani SM, Herri JM (2019) Cyclopentane hydrates-a candidate for desalination? J Environ Chem Eng 7:103359
130. Erfani A, Varaminian F (2016) Kinetic promotion of non-ionic surfactants on cyclopentane hydrate formation. J Mol Liq 221:963–971
131. Brown EP, Koh CA (2016) Micromechanical measurements of the effect of surfactants on cyclopentane hydrate shell properties. Phys Chem Chem Phys 18:594–600
132. Henry D, Gilles B, Jean-Philippe T, Christophe, D, Philippe G (2019) Evaluation of the performance of a new biodegradable AA-LDHI in cyclopentane hydrate and CH4/C3H8 gas hydrate systems. SPE Middle East Oil Gas Show Conf. MEOS, Proc, 2019-March, pp 1–13

133. Linga P, Kumar R, Englezos P (2007) Gas hydrate formation from hydrogen/carbon dioxide and nitrogen/carbon dioxide gas mixtures. Chem Eng Sci 62:4268–4276
134. Kumar R, Linga P, Englezos P (2006) Pre post combustion capture of carbon dioxide via hydrate formation. IEEE EIC Clim Chang Technol Conf EICCCC 2006:1–7
135. Xu CG, Li X (2014) Sen Research progress of hydrate-based CO_2 separation and capture from gas mixtures. RSC Adv 4:18301–18316
136. Ho LC, Babu P, Kumar R, Linga P (2013) HBGS (hydrate based gas separation) process for carbon dioxide capture employing an unstirred reactor with cyclopentane. Energy 63:252–259
137. da Lirio CFS, Pessoa FLP, Uller AMC (2013) Storage capacity of carbon dioxide hydrates in the presence of sodium dodecyl sulfate (SDS) and tetrahydrofuran (THF). Chem Eng Sci 96:118–123
138. Jiang, L. Le, Li AR, Xu JF, Liu YJ (2016) Effects of SDS and SDBS on CO2Hydrate formation, induction time, storage capacity and stability at 274.15 K and 5.0 MPa. Chem Select 1:6111–6114
139. Yang M, Liu W, Song Y, Ruan X, Wang X, Zhao J, Jiang L, Li Q (2013) Effects of additive mixture (THF/SDS) on the thermodynamic and kinetic properties of CO2/H2 hydrate in porous media. Ind Eng Chem Res 52:4911–4918
140. Song Y, Wang X, Yang M, Jiang L, Liu Y, Dou B, Zhao J, Wang S (2013) Study of selected factors affecting hydrate-based carbon dioxide separation from simulated fuel gas in porous media. Energy Fuels 27:3341–3348
141. Pandey JS, von Solms N (2019) Hydrate stability and methane recovery from gas hydrate through CH_4–CO_2 replacement in different mass transfer scenarios. Energies 12:2309
142. Frankcombe TJ, Kroes GJ (2007) Molecular dynamics simulations of type-sII hydrogen clathrate hydrate close to equilibrium conditions. J Phys Chem C 111:13044–13052
143. Struzhkin VV, Militzer B, Mao WL, Mao HK, Hemley RJ (2007) Hydrogen storage in molecular clathrates. Chem Rev 107:4133–4151
144. Ozaki M, Tomura S, Ohmura R, Mori YH (2014) Comparative study of large-scale hydrogen storage technologies: Is hydrate-based storage at advantage over existing technologies? Int J Hydrogen Energy 39:3327–3341
145. Trueba AT, Radović IR, Zevenbergen JF, Kroon MC, Peters CJ (2012) Kinetics measurements and in situ Raman spectroscopy of formation of hydrogen-tetrabutylammonium bromide semi-hydrates. Int J Hydrogen Energy 37:5790–5797
146. Veluswamy HP, Chin WI, Linga P (2014) Clathrate hydrates for hydrogen storage: The impact of tetrahydrofuran, tetra-n-butylammonium bromide and cyclopentane as promoters on the macroscopic kinetics. Int J Hydrogen Energy 39:16234–16243
147. Du J, Wang L, Liang D, Li D (2012) Phase equilibria and dissociation enthalpies of hydrogen semi-clathrate hydrate with tetrabutyl ammonium nitrate. J Chem Eng Data 57:603–609
148. Florusse LJ, Peters CJ, Schoonman J, Hester KC, Koh CA, Dec SF, Marsh KN, Sloan ED (2004) Stable low-pressure hydrogen clusters stored in a binary clathrate hydrate. Science (80-.) 306:469–471
149. Veluswamy HP, Linga P (2013) Macroscopic kinetics of hydrate formation of mixed hydrates of hydrogen/tetrahydrofuran for hydrogen storage. Int J Hydrogen Energy 38:4587–4596
150. Alavi S, Ripmeester JA (2007) Hydrogen-gas migration through clathrate hydrate cages. Angew. Chemie—Int. Ed. 46:6102–6105
151. Okuchi T, Moudrakovski IL, Ripmeester JA (2007) Efficient storage of hydrogen fuel into leaky cages of clathrate hydrate. Appl Phys Lett 91:2005–2008
152. Kumar R, Klug DD, Ratcliffe CI, Tulk CA, Ripmeester JA (2013) Low-pressure synthesis and characterization of hydrogen-filled ice Ic. Angew Chemie—Int Ed 52:1531–1534
153. Lu H, Wang J, Liu C, Ratcliffe CI, Becker U, Kumar R, Ripmeester J (2012) Multiple H 2 occupancy of cages of clathrate hydrate under mild conditions. J Am Chem Soc 134:9160–9162
154. Grim RG, Kerkar PB, Sloan ED, Koh CA, Sum AK (2012) Rapid hydrogen hydrate growth from non-stoichiometric tuning mixtures during liquid nitrogen quenching. J Chem Phys 136

155. Veluswamy HP, Chen JY, Linga P (2015) Surfactant effect on the kinetics of mixed hydrogen/propane hydrate formation for hydrogen storage as clathrates. Chem Eng Sci 126:488–499
156. Di Profio P, Arca S, Rossi F, Filipponi M (2009) Comparison of hydrogen hydrates with existing hydrogen storage technologies: energetic and economic evaluations. Int J Hydrogen Energy 34:9173–9180
157. Veluswamy HP, Hong QW, Linga P (2016) Morphology study of methane hydrate formation and dissociation in the presence of amino acid
158. Carter BO, Wang W, Adams DJ, Cooper AI (2010) Gas storage in "Dry Water" and "Dry Gel" clathrates. Langmuir 26:3186–3193
159. Liu Y, Chen B, Chen Y, Zhang S, Guo W, Cai Y, Tan B, Wang W (2015) Methane storage in a hydrated form as promoted by leucines for possible application to natural gas transportation and storage. Energy Technol 3:815–819
160. Scott MJ, Jones MN (2000) The biodegradation of surfactants in the environment. Biochim Biophys Acta—Biomembr 1508:235–251
161. Campbell JM (1992) Gas conditioning and processing, vol 2. The equipment modules, ISBN 0-9703449-0-2
162. Sloan ED, Koh CA (2007) Clathrate hydrates of natural gases, 3rd edn, ISBN 9781420008494
163. Carroll J (2014) Natural gas hydrates—a guide for engineers, 3rd edn, ISBN 978-0-12-800074-8
164. Anderson BJ, Tester JW, Borghi GP, Trout BL (2005) Properties of inhibitors of methane hydrate formation via molecular dynamics simulations. J Am Chem Soc 127:17852–17862
165. Xiao C, Adidharma H (2009) Dual function inhibitors for methane hydrate. Chem Eng Sci 64:1522–1527
166. Kelland MA, Moi N, Howarth M (2013) Breakthrough in synergists for kinetic hydrate inhibitor polymers, hexaalkylguanidinium salts: Tetrahydrofuran hydrate crystal growth inhibition and synergism with polyvinylcaprolactam. Energy Fuels
167. Sa JH, Kwak GH, Lee BR, Park DH, Han K, Lee KH (2013) Hydrophobic amino acids as a new class of kinetic inhibitors for gas hydrate formation. Sci Rep 3:1–7
168. Lee D, Go W, Seo Y (2019) Experimental and computational investigation of methane hydrate inhibition in the presence of amino acids and ionic liquids. Energy
169. Klamt A (1995) Conductor-like screening model for real solvents: a new approach to the quantitative calculation of solvation phenomena. J Phys Chem
170. Eckert F, Klamt A (2002) Fast solvent screening via quantum chemistry: COSMO-RS Approach. AIChE J
171. Klamt A, Eckert F, Arlt W (2010) COSMO-RS: an Alternative to simulation for calculating thermodynamic properties of liquid mixtures. Annu Rev Chem Biomol Eng
172. Klamt A, Schüürmann G (1993) COSMO: a new approach to dielectric screening in solvents with explicit expressions for the screening energy and its gradient. J Chem Soc Perkin Trans 2
173. Dickens GR, Quinby-Hunt MS (1997) Methane hydrate stability in pore water: A simple theoretical approach for geophysical applications. J Geophys Res B Solid Earth 102:773–783
174. Kirkwood JG (1934) Theory of solutions of molecules containing widely separated charges with special application to zwitterions. J Chem Phys
175. Nashed O, Dadebayev D, Khan MS, Bavoh CB, Lal B, Shariff AM (2018) Experimental and modelling studies on thermodynamic methane hydrate inhibition in the presence of ionic liquids. J Mol Liq
176. Pieroen AP (1955) Gas hydrates—approximate relations between heat of formation, composition and equilibrium temperature lowering by "inhibitors". Recl des Trav Chim des Pays-Bas 74:995–1002
177. Partoon B, Wong NMS, Sabil KM, Nasrifar K, Ahmad MR (2013) A study on thermodynamics effect of [EMIM]-Cl and [OH-C2MIM]-Cl on methane hydrate equilibrium line. Fluid Phase Equilib

178. Javanmardi J, Moshfeghian M, Maddox RN (1998) Simple method for predicting gas-hydrate-forming conditions in aqueous mixed-electrolyte solutions. Energy Fuels 12:219–222
179. Javanmardi J, Moshfeghian M, Maddox RN (2001) An accurate model for prediction of gas hydrate formation conditions in mixtures of aqueous electrolyte solutions and alcohol. Can J Chem Eng 79:367–373
180. Bavoh CB, Partoon B, Lal B, Gonfa G, Foo Khor S, Sharif AM (2017) Inhibition effect of amino acids on carbon dioxide hydrate. Chem Eng Sci 171:331–339
181. Xiao C, Wibisono N, Adidharma H (2010) Dialkylimidazolium halide ionic liquids as dual function inhibitors for methane hydrate. Chem Eng Sci 65:3080–3087
182. Atilhan M, Pala N, Aparicio S (2014) A quantum chemistry study of natural gas hydrates. J Mol Model 20:1–15
183. Tariq M, Atilhan M, Khraisheh M, Othman E, Castier M, García G, Aparicio S, Tohidi B (2016) Experimental and DFT approach on the determination of natural gas hydrate equilibrium with the use of excess N_2 and choline chloride ionic liquid as an inhibitor. Energy Fuels 30:2821–2832
184. Choudhary N, Das S, Roy S, Kumar R (2016) Effect of polyvinylpyrrolidone at methane hydrate-liquid water interface. Application in flow assurance and natural gas hydrate exploitation. Fuel 186:613–622
185. Mohamed NA, Tariq M, Atilhan M, Khraisheh M, Rooney D, Garcia G, Aparicio S (2017) Investigation of the performance of biocompatible gas hydrate inhibitors via combined experimental and DFT methods. J Chem Thermodyn 111:7–19
186. Bellucci MA, Walsh MR, Trout BL (2018) Molecular dynamics analysis of anti-agglomerant surface adsorption in natural gas hydrates 122
187. Fang B, Ning F, Hu S, Guo D, Ou W, Wang C, Wen J, Sun J, Liu Z, Koh CA (2020) The effect of surfactants on hydrate particle agglomeration in liquid hydrocarbon continuous systems: a molecular dynamics simulation study. RSC Adv 10:31027–31038
188. Bhattacharjee G, Choudhary N, Barmecha V, Kushwaha OS, Pande NK, Chugh P, Roy S, Kumar R (2019) Methane recovery from marine gas hydrates: a bench scale study in presence of low dosage benign additives. Appl Energy 253:113566
189. Sammalkorpi M, Karttunen M, Haataja M (2007) Structural properties of ionic detergent aggregates: a large-scale molecular dynamics study of sodium dodecyl sulfate. J Phys Chem B 111:11722–11733
190. Chun BJ, Choi JIl, Jang SS (2015) Molecular dynamics simulation study of sodium dodecyl sulfate micelle: Water penetration and sodium dodecyl sulfate dissociation. Colloids Surfaces A Physicochem Eng Asp 474:36–43
191. Kitabata M, Fujimoto K, Yoshii N, Okazaki S (2016) A molecular dynamics study of local pressures and interfacial tensions of SDS micelles and dodecane droplets in water. J Chem Phys 144:224701
192. Bresme F, Faraudo J (2004) Computer simulation studies of newton black films. Langmuir 20:5127–5137
193. Hande VR, Chakrabarty S (2016) Exploration of the presence of bulk-like water in AOT reverse micelles and water-in-oil nanodroplets: the role of charged interfaces, confinement size and properties of water. Phys Chem Chem Phys 18:21767–21779
194. Volkov NA, Tuzov NV, Shchekin AK (2016) Molecular dynamics study of salt influence on transport and structural properties of SDS micellar solutions. Fluid Phase Equilib 424:114–121
195. Poghosyan AH, Arsenyan LH, Gharabekyan HH, Falkenhagen S, Koetz J, Shahinyan AA (2011) Molecular dynamics simulations of inverse sodium dodecyl sulfate (SDS) micelles in a mixed toluene/pentanol solvent in the absence and presence of poly(diallyldimethylammonium chloride) (PDADMAC). J Colloid Interface Sci 358:175–181
196. Poghosyan AH, Arsenyan LH, Shahinyan AA, Koetz J (2016) Polyethyleneimine loaded inverse SDS micelle in pentanol/toluene media. Colloids Surf A Physicochem Eng Asp 506:402–408

197. Fujimoto K, Yoshii N, Okazaki S (2012) Free energy profiles for penetration of methane and water molecules into spherical sodium dodecyl sulfate micelles obtained using the thermodynamic integration method combined with molecular dynamics calculations. J Chem Phys 136:014511
198. Fujimoto K, Yoshii N, Okazaki S (2012) Molecular dynamics study of free energy of transfer of alcohol and amine from water phase to the micelle by thermodynamic integration method. J Chem Phys 137:094902
199. Brodskaya EN (2012) Computer simulations of micellar systems. Colloid J 74:154–171
200. Kinning DJ, Winey KI, Thomas EL (1988) Structural transitions from spherical to nonspherical micelles in blends of poly(styrene-butadiene) diblock copolymer and polystyrene homopolymers. Macromolecules 21:3502–3506
201. Choudhary N, Hande VR, Roy S, Chakrabarty S, Kumar R (2018) Effect of sodium dodecyl sulfate surfactant on methane hydrate formation: a molecular dynamics study. J Phys Chem B 122:6536–6542
202. Khurana M, Yin Z, Linga P (2017) A review of clathrate hydrate nucleation. ACS Sustain Chem Eng 5:11176–11203
203. Walsh MR, Koh CA, Sloan DE, Sum AK, Wu DT (2009) Microsecond simulations of spontaneous methane hydrate nucleation and growth. Science (80-.) 326:1095–1098
204. Michalis VK, Tsimpanogiannis IN, Stubos AK, Economou IG (2016) Direct phase coexistence molecular dynamics study of the phase equilibria of the ternary methane-carbon dioxide-water hydrate system. Phys Chem Chem Phys 18:23538–23548
205. Kumar A, Veluswamy HP, Linga P, Kumar R (2019) Molecular level investigations and stability analysis of mixed methane-tetrahydrofuran hydrates: implications to energy storage. Fuel 236:1505–1511
206. Carver TJ, Drew MGB, Rodger PM (1995) Inhibition of crystal growth in methane hydrate. J Chem Soc, Faraday Trans 91:3449–3460
207. Mehrabian H, Bellucci MA, Walsh MR, Trout BL (2018) Effect of Salt on Antiagglomerant Surface Adsorption in Natural Gas Hydrates. J Phys Chem C 122:12839–12849
208. Mehrabian H, Walsh MR, Trout BL (2019) In Silico Analysis of the Effect of Alkyl Tail Length on Antiagglomerant Adsorption to Natural Gas Hydrates in Brine. J Phys Chem C 123:17239–17248
209. Jiménez-Ángeles F, Firoozabadi A (2018) Hydrophobic hydration and the effect of NaCl salt in the adsorption of hydrocarbons and surfactants on clathrate hydrates. ACS Cent Sci 4:820–831
210. Naullage PM, Bertolazzo AA, Molinero V (2019) How do surfactants control the agglomeration of clathrate hydrates?. ACS Cent, Sci
211. Bavoh CB, Lal B, Nashed O, Khan MS, Keong LK, Bustam MA (2016) COSMO-RS: An ionic liquid prescreening tool for gas hydrate mitigation. *Chinese J. Chem. Eng*
212. Klamt A, Eckert F (2000) COSMO-RS: a novel and efficient method for the a priori prediction of thermophysical data of liquids. Fluid Phase Equilib 172:43–72
213. Klamt A, Eckert F, Hornig M, Beck ME, Brger T (2002) Prediction of aqueous solubility of drugs and pesticides with COSMO-RS. J Comput Chem 23:275–281
214. Klamt A (2012) Solvent-screening and co-crystal screening for drug development with COSMO-RS. J Cheminform 4:1–2
215. Paduszyński K (2017) An overview of the performance of the COSMO-RS approach in predicting the activity coefficients of molecular solutes in ionic liquids and derived properties at infinite dilution. Phys Chem Chem Phys 19:11835–11850
216. Xia L, Wang J, Liu S, Li Z, Pan H (2019) Prediction of CO_2 solubility in ionic liquids based on multi-model fusion method. Processes 7:258